Aus der Klinik für Neurochirurgie
der Heinrich-Heine-Universität Düsseldorf
Komm. Direktor: Univ.-Prof. Dr. med. Jan Frederick Cornelius

A Novel Comprehensive Protocol for Establishing a Circle of Willis Perforation Mouse Model and Assessing Severity After Subarachnoid Hemorrhage

Dissertation

zur Erlangung des Grades eines Doktors der Medizin
der Medizinischen Fakultät der Heinrich-Heine-Universität Düsseldorf

vorgelegt von
Rui Zhang
Düsseldorf, 2024

Als Inauguraldissertation gedruckt mit Genehmigung der

Medizinischen Fakultät der Heinrich-Heine-Universität Düsseldorf

gez.:

Dekan: Prof. Dr. med. Nikolaj Klöcker

Erstgutachter: Prof.Dr.med Sajjad Muhammad

Zweitgutachter: PD.Dr.Michael Gliem

Dedication

I dedicate this work to science, democracy, and freedom, which form the fundamental pillars of human civilization.

Publications

1. **Zhang R**, Khan D, Muhammad S. Establishment of a novel protocol for assessing the severity of subarachnoid hemorrhage in circle Willis perforation mouse model. Sci Rep. 2024;14(1):10147.

2. **Zhang R**, Muhammad S. Surgical repair of torn base of ruptured middle cerebral artery trifurcation aneurysm. Acta Neurochir (Wien). 2024;166(1):148.

3. Muhammad S, **Zhang R**, Filler T, Hanggi D, Meling TR. Trans-lateral ventricular approach for surgical treatment of high-located P2-P3 junction posterior cerebral artery aneurysms: from anatomical research to clinical application. Acta Neurochir (Wien). 2024;166(1):50.

Zusammenfassung

Diese Studie stellt neuartige Methoden vor, die darauf abzielen, die Zugänglichkeit und Reproduzierbarkeit der Induktion einer Subarachnoidalblutung (SAB) in murinen Modellen zu verbessern und die mit den aktuellen Techniken verbundenen Herausforderungen anzugehen. Erstens wird ein neuer chirurgischer Ansatz zur Induktion von SAB vorgeschlagen, der eine direkte Punktion der A. carotis communis (CCA) beinhaltet, um das Verfahren zu vereinfachen und die anatomische Integrität zu erhalten. Diese Modifikation zielt darauf ab, die Lernkurve der traditionellen Methoden zu reduzieren und gleichzeitig die experimentelle Strenge aufrechtzuerhalten. Zweitens wird ein neuartiger Bewertungsscore für die Neurologische Schwere nach SAB (ROB-Score) etabliert, um die Schwere der SAB quantitativ zu bewerten und die Konsistenz in präklinischen Studien sicherzustellen. Dieses Bewertungssystem integriert objektive Parameter wie die Leistung im offenen Feldtest, die Ergebnisse des Rotarod-Tests und Messungen des Körpergewichts, um eine umfassende Bewertung der post-SAB-neurologischen Defizite zu ermöglichen. Zusammen bieten diese Fortschritte vielversprechende Ansätze für verbesserte SAB-Forschungsmethoden, erleichtern effizientere präklinische Studien und beschleunigen die Entwicklung therapeutischer Interventionen.

Summary

This study introduces novel methodologies aimed at enhancing the accessibility and reproducibility of subarachnoid hemorrhage (SAH) induction in murine models, addressing the challenges associated with current techniques. Firstly, a new surgical approach for SAH induction, involving direct puncturing of the common carotid artery (CCA), is proposed to simplify the procedure and preserve anatomical integrity. This modification aims to reduce the learning curve associated with traditional methods while maintaining experimental rigor. Secondly, a novel Post SAH Neurological Severity Assessment Score (ROB score) is established to quantitatively assess SAH severity and ensure consistency in preclinical studies. This scoring system integrates objective parameters such as open-field test performance, rotarod test results, and body weight loss measurements to provide a comprehensive evaluation of post-SAH neurological deficits. Together, these advancements offer promising avenues for improved SAH research methodologies, facilitating more efficient preclinical studies and accelerating the development of therapeutic interventions.

List of Abbreviation:

ACA: Anterior Cerebral Artery

BWL: Body Weight Loss

cWp: Circle of Willis Perforation

CCA: Common Carotid Artery

CT: Computer Tomography

CVS: Cerebral Vasospasm

DCI: Delayed Cerebral Ischemia

DIND: Delayed Ischemic Neurological Deficit

EBI: Early Brain Injury

ECA: External Carotid Artery

FPS: Frames Per Second

GCS: Glasgow Coma Scale

ICA: Internal Carotid Artery

ICP: Intracranial Pressure

MCA: Middle Cerebral Artery

MCAO: Middle Cerebral Artery Occlusion

MRI: Magnetic Resonance Imaging

OA: Occipital Artery

PPA: Pterygopalatine Artery

RPM: Rotations Per Minute

SAH: Subarachnoid Hemorrhage

aSAH: Aneurysmal Subarachnoid Hemorrhage

Table of Contents

1. Introduction

1.1. Subarachnoid Hemorrhage

Subarachnoid hemorrhage (SAH) is a pathological condition characterized by the release of blood from a normal artery into the subarachnoid space (1). Typically associated with traumatic brain injury or intracranial vascular disease, our study focuses primarily on spontaneous SAH resulting from the rupture of aneurysms or arteriovenous malformations.

As evidenced by previous studies, the majority of spontaneous SAH cases are linked to the rupture of intracranial aneurysms (2). It is noteworthy to mention that the morbidity incidences observed in North European and Japanese populations compared to other nations (3). Normally to say, the Incidences per 100 000 person-years were 22.7 (95% CI 21.9 to 23.5) in Japan, 19.7 (18.1 to 21.3) in Finland, 4.2 (3.1 to 5.7) in South and Central America, and 9.1 (8.8 to 9.5) in the other regions. Currently, the world wide incidence of SAH is around 10 per 100,000 and decreasing in recent years (4).

The mortality rate for SAH is approximately 30% or even higher to 50%, emphasizing the severity of this condition (5)(6)(7). Furthermore, survivors often experience varying degrees of deficits. These challenges encompass deficits in memory, executive function, attention and concentration, psychomotor speed, and language, as well as heightened levels of anxiety and depression (8).The prevalence of these outcomes underscores the importance of understanding and addressing the factors contributing to the occurrence and consequences of spontaneous SAH.

1.2. Early Brain Injury

Early brain injury (EBI) is the early event within first hours and days after subarachnoid hemorrhage and plays a crucial role in the context of SAH, particularly

in understanding the immediate neurological consequences following the rupture of an intracranial aneurysm (9). The rupture of an intracranial aneurysm leading to subarachnoid hemorrhage initiates a sequence of events, collectively forming early brain injury (EBI), which in turn shapes the subsequent progression of damage and influences patient outcomes (10).

In the aftermath of an aneurysm rupture, blood enters the subarachnoid space, leading to elevated intracranial pressure, reduced cerebral blood flow, and ischemic damage to surrounding tissues (11). EBI encompasses these acute pathophysiological changes occurring within the first hours and days after the hemorrhagic event (12).

Key mechanisms contributing to EBI in SAH include oxidative stress, inflammation, blood-brain barrier disruption, and excitotoxicity. These processes can result in secondary brain injury, exacerbating the initial damage caused by the aneurysm rupture (13)(14)(15).

Consequently, understanding and targeting EBI have become crucial aspects of therapeutic strategies aimed at improving outcomes for SAH patients. Research efforts focus on identifying biomarkers, imaging modalities, and interventions that can effectively mitigate EBI and its cascading effects. By unraveling the complexities of EBI in the SAH context, clinicians and researchers strive to develop more targeted and early interventions to improve patient prognosis and long-term neurocognitive outcomes.

1.3. Delayed Ischemic Neurological Deficit and Delayed Cerebral Ischemia

Delayed Ischemic Neurological Deficit (DIND) is a significant complication that can arise in the aftermath of subarachnoid hemorrhage, particularly following early EBI. DIND typically manifests days after the initial bleeding event and is characterized by a decline in neurological function, often attributed to delayed cerebral ischemia (DCI) (16)(17).

The pathophysiology of DIND/DCI is intricate and involves a multitude of factors. It encompasses a blend of vasospasm, inflammation, impaired autoregulation, and additional secondary processes that collectively contribute to the compromise of blood flow to the brain (18). One key contributor is cerebral vasospasm, a phenomenon where the blood vessels constrict, reducing blood supply to vital brain regions (19).

Monitoring and predicting DIND/DCI pose significant challenges and various clinical, radiological, and laboratory parameters are studied to identify individuals at risk. Neurological assessments, imaging studies such as angiography, and measurement of biomarkers may be employed to detect early signs of DIND (20)(21)(22).

Essential aspects of patient care for SAH involve the prevention and management of DCI. This includes strategies such as ensuring optimal cerebral perfusion, administering nimodipine to avert vasospasm, and addressing underlying factors like electrolyte imbalances (21)(23).

Research efforts are ongoing to explore new therapeutic avenues and improve prognostic tools for DCI, aiming to enhance patient outcomes in the challenging context of SAH.

1.4. Post SAH Inflammation

Post-SAH inflammation serves as a crucial link between the initial insult of EBI and the development of DCI. Following the hemorrhagic event, a cascade of inflammatory processes is triggered, contributing significantly to the pathophysiology of SAH (15)(24).

The inflammatory response encompasses the activation of immune cells, the release of cytokines, and the recruitment of inflammatory mediators (25). This inflammatory milieu not only exacerbates the damage caused by the initial hemorrhage but also plays a pivotal role in subsequent complications, including

cerebral vasospasm (CVS) and delayed neurological deficits (26).

The activated inflammatory pathways contribute to endothelial dysfunction, blood-brain barrier disruption, and the release of vasoactive substances, all of which collectively contribute to compromised cerebral perfusion. The resultant vascular changes, in conjunction with other pathophysiological factors, contribute to the occurrence of DCI (27).

Understanding the dynamics of post-SAH inflammation is crucial for developing targeted therapeutic interventions. Anti-inflammatory strategies aimed at mitigating the excessive immune response and its downstream effects are under investigation to potentially attenuate the progression from EBI to DCI.

1.5. Animal model for SAH research

SAH research relies on animal models to unravel the complex pathophysiology of this devastating neurological condition. Various species have been utilized, each offering unique advantages and challenges. Choosing an appropriate model involves carefully balancing anatomical relevance, experimental feasibility, and ethical considerations (28).

1.5.1. Non-Rodent Models

Primates: Primates, particularly monkeys, have been employed to study SAH due to their closer physiological resemblance to humans. However, ethical considerations, cost, and limited availability restrict their widespread use (29)(30).

Large Mammals: Large mammalian models, such as porcine models (pigs), canine models (dogs), and feline models (cats), present notable advantages owing to their anatomical and physiological resemblances to humans. Pigs, in particular, have been preferred due to their vascular similarities (31). However, these models pose challenges, including elevated costs, ethical considerations, and practical limitations (32).

Rabbits: Rabbits have been used to study SAH due to their relatively low cost,

ease of handling, and accessibility (33). While they do not precisely mimic human physiology, their use allows for controlled experiments and insights into certain aspects of SAH pathology (34).

1.5.2. Rodent Models

Among rodent models, mice, and rats are the most extensively employed for SAH research. Their genetic manipulability, cost-effectiveness, and well-established methodologies make them attractive choices. Common induction methods involve: direct injection of blood into the cisterna magna (35) or into the pre-chiasmatic cistern (36), tearing an intracisternal vein (37), or perforating the Circle of Willis (cWp) using an endovascular filament inserted through the external carotid artery(ECA) (38)(39).

1.5.3. Advantages of Rodent Models

Genetic Manipulation: Rodent models permit genetic modifications, facilitating the study of specific molecular pathways and gene functions in SAH pathology.

Cost-Effectiveness: Compared to larger mammals, rodents are cost-effective, enabling larger sample sizes for statistical robustness.

Well-Characterized Techniques: Established methods for SAH induction, including endovascular perforation and blood injection, ensure reproducibility and consistency across studies (39)(40).

1.5.4. Challenges and Considerations

Anatomical Differences: Rodents have anatomical differences compared to humans, impacting the translation of findings. Researchers must carefully interpret and extrapolate results to human scenarios.

Size Limitations: The smaller size of rodents may limit certain experimental procedures and imaging capabilities.

Species-Specific Responses: Rodents may exhibit species-specific responses to

SAH, necessitating careful interpretation of results (41).

In summary animal models play a crucial role in advancing our understanding of SAH. While larger mammals offer physiological similarities, rodents, particularly mice and rats, stand out for their practicality, cost-effectiveness, and genetic manipulability. As SAH research progresses, the collective insights from diverse animal models contribute to a more comprehensive understanding of this intricate neurological disorder.

1.6. Injection Mouse Model

1.6.1. Summary Insight of The Injection Model

The blood injection model, a frequently employed method for inducing SAH in mice, encompasses both single and double injection variations. Through direct injections of autologous blood, researchers can target specific sites, such as the cisterna magna or the pre-chiasmatic cistern. While providing controlled and reproducible means for studying SAH, it is essential to acknowledge the model's limitations in fully mimicking the natural processes of spontaneous SAH. The single injection model allows researchers to modulate SAH severity by adjusting blood volume, while the double injection model provides insights into delayed effects. Despite these advantages, the model's inability to fully replicate spontaneous SAH processes should be considered when interpreting findings. The controlled settings of the blood injection model facilitate comprehensive neurobehavioral assessments, offering valuable insights into both immediate and delayed consequences post-SAH. This model, with its strengths and constraints, remains a valuable tool for in-depth studies, contributing to our understanding of SAH pathophysiology (35)(36)(42).

1.6.2. Surgical Procedure of Cisterna Magna Injection Model

Anesthesia: Mice are anesthetized to ensure immobility and minimize stress during the procedure. Commonly used anesthetics include isoflurane inhalation or a

combination of ketamine and xylazine intraperitoneal injection.

Surgical Exposure: A midline incision is made at the back of the neck to expose the cisterna magna, a cerebrospinal fluid-filled space at the base of the brain.

Blood Collection: Autologous blood is typically collected from the tail artery or the femoral artery. The collected blood is then loaded into a micro syringe for injection.

Injection: Using a micro needle attached to the micro syringe, a predetermined volume of blood is injected into the cisterna magna. The injection is performed slowly and steadily to avoid sudden increases in intracranial pressure.

Closure: Following blood injection, the incision is closed, and the mouse is allowed to recover (35).

1.6.3. Single Injection Model:

In this variant, a single injection of autologous blood is administered into either the cisterna magna or the pre-chiasmatic cistern, allowing researchers to modulate the severity of SAH by adjusting the injected blood volume (43).

1.6.4. Double Injection Model:

The double injection model involves two sequential injections, often into the cisterna magna. This approach allows for a more prolonged exposure to blood, potentially capturing delayed effects and providing insights into the evolving pathophysiology of SAH (44).

1.7. Perforation Mouse Model

1.7.1. Summary Insight of The Perforation Mouse Model

Perforation mouse models in SAH research offer diverse approaches, notably the craniotomy vein model and the Circle of Willis perforation (cWp) model. In the

craniotomy vein model, a localized hemorrhagic insult is induced by perforating a cortical vein following a small craniotomy. This model provides insights into the consequences of hemorrhage from specific brain regions. On the other hand, the cWp model involves navigating a filament into the internal carotid artery (ICA) to induce SAH, simulating a more broader subarachnoid hemorrhagic insult. This approach potentially resembles spontaneous SAH scenarios more closely (38)(39).

1.7.2. Surgical Procedure of The cWp Mouse Model

In the cWp model, a mouse is anesthetized and positioned supine, and a midline incision is made in the neck to expose the salivary glands, trachea, and muscles. After careful dissection of the salivary glands, the ECA and ICA are identified, and the ECA is separated from the ICA to create space for filament insertion. A filament, typically made of nylon, is gently advanced through the ECA into the ICA, and the vessel wall is delicately perforated to induce SAH. Following SAH induction, the filament is withdrawn, and the incision is closed with sutures. The mouse is allowed to recover, and postoperative care is provided, including monitoring for signs of distress or neurological deficits. The cWp model offers a controlled method for inducing SAH while minimizing surgical complexity, allowing researchers to study the consequences of a systemic hemorrhagic insult.

The cWp model has become the predominant choice among perforation mouse models in SAH research, given its capacity to replicate a systemic hemorrhagic insult with a relatively straightforward surgical procedure. This targeted perforation effectively induces SAH, enabling researchers to investigate the consequences of a systemic hemorrhagic event. The preference for the cWp model is justified by its ability to emulate crucial aspects of SAH, while simultaneously streamlining the surgical process compared to more intricate methods like the craniotomy vein model. The choice between these models depends on research objectives, considering factors such as anatomical targets, surgical complexity, and the desired extent of mimicry of natural SAH processes. Both models contribute distinct perspectives, collectively

enhancing our understanding of SAH pathophysiology and the consequences of hemorrhagic insults in different anatomical contexts (37)(38)(39).

1.8. Post-SAH Neurological Deficit Assessment

1.8.1. Rotarod Test

The rotarod test is a widely employed and versatile behavioral assessment utilized in rodent research to evaluate motor coordination, balance, and endurance. This test provides valuable insights into the motor function of rodents and is particularly useful for studying various neurological disorders, assessing the effects of drugs, and evaluating the impact of experimental interventions (45).

In the rotarod test, animals, usually mice or rats, are placed on a rotating rod, and their ability to maintain balance and coordination is assessed as the rod accelerates. The test offers a dynamic and controlled environment to observe motor performance, allowing researchers to gauge how well animals adapt to the changing conditions. This adaptability is crucial for assessing motor learning and memory (46).

The versatility of the rotarod test extends to its ability to measure both acute and chronic changes in motor performance. Acute changes can be indicative of immediate effects of treatments or interventions, while the assessment of chronic changes allows for the observation of motor deficits or improvements over an extended period. This longitudinal aspect makes the rotarod test particularly valuable for tracking the progression or recovery of motor function in response to various experimental conditions (47).

Researchers commonly use the rotarod test in preclinical studies to elucidate the impact of neurological conditions or interventions on motor behavior. The test's sensitivity to subtle motor impairments makes it a reliable tool for assessing the efficacy of potential therapeutic strategies. Additionally, the rotarod test can be adapted to specific experimental needs, such as assessing the influence of genetic

factors, drug treatments, or environmental enrichment on motor performance (48).

1.8.2. Open-field Test

The open field test is a commonly used behavioral assay in rodent research designed to assess general locomotor activity, exploration, and anxiety-related behaviors. In this test, animals, typically mice or rats, are placed in a novel and open arena, and their spontaneous movements and exploratory behaviors are observed and quantified. The open field test provides insights into the baseline activity levels of rodents, their willingness to explore new environments, and their anxiety-like responses to the exposed and unfamiliar surroundings (49).

During the test, parameters such as total distance traveled, time spent in different zones of the arena, and rearing behavior are measured. Increased locomotor activity, extended exploration, and heightened rearing can be indicative of reduced anxiety-like behaviors, while decreased activity and limited exploration may suggest heightened anxiety levels (50)(51).

The open field test proves instrumental in examining how genetic modifications, pharmacological interventions, or environmental variables influence the emotional responses and exploratory behaviors of rodents (52).

This test's simplicity and ability to provide multifaceted information make it a versatile tool in preclinical studies. Researchers can use the open field test to investigate the impact of various interventions on emotional responses and locomotor activity, contributing to a comprehensive understanding of factors influencing rodent behavior in novel environments.

1.8.3. Body Weight Loss Monitoring

Monitoring body weight loss is a crucial parameter in assessing post-SAH outcomes in rodents. The dynamic changes in body weight serve as a sensitive indicator of the overall health and well-being of the animals following SAH

induction.

Significant and sustained weight loss can signal the severity of the physiological impact and the potential development of secondary complications. This parameter is particularly valuable as it reflects the systemic consequences of SAH, including potential effects on appetite, metabolism, and overall physiological stress.

Researchers often incorporate regular body weight measurements into post-SAH assessment protocols to track the progression of recovery or the persistence of adverse effects. This holistic approach provides essential insights into the overall health status of the rodents, aiding in the comprehensive evaluation of SAH-induced physiological changes and the efficacy of interventions (53)(54).

1.8.4. Post SAH Neurological Evaluation Score

Neurological scoring systems play a pivotal role in characterizing the extent of neurological deficits in mouse models of SAH. These systems provide a quantitative and standardized approach to evaluate a spectrum of neurological functions, encompassing motor abilities, coordination, reflexes, and sensory perception. By employing well-established scoring scales, researchers can systematically assess the severity of neurological impairments, facilitating the characterization of SAH-induced damage and the evaluation of potential therapeutic interventions (55).

Modified Garcia Score: The modified Garcia score is a widely utilized neurological scoring system that evaluates various functional domains, including spontaneous activity, symmetry of limb movement, forepaw outstretching, climbing, body proprioception, and response to vibrissae touch. Each parameter is assigned a score, and the cumulative result provides a comprehensive assessment of overall neurological function. Lower scores indicate more severe deficits (56) (Table. 1).

Bederson Score: Developed specifically for ischemic stroke models but adapted for SAH studies, the Bederson score primarily focuses on evaluating motor function and global neurological status. The scale assigns scores based on observable

behaviors, such as circling behavior, forelimb flexion, and resistance to lateral push. Higher scores on the Bederson scale indicate greater neurological impairment. Researchers commonly integrate the Bederson score with other behavioral assessments for a comprehensive evaluation of neurological outcomes (57) (Table. 2).

Neurological Severity Score (NSS): The Neurological Severity Score (NSS) is a comprehensive scoring system that evaluates a range of neurological functions, encompassing motor coordination, balance, alertness, and physiological behavior (Table. 3). It often incorporates tasks such as beam balance, reflexes, and general behavior. A higher NSS reflects more severe neurological deficits (58).

In summary neurological scoring systems offer a standardized approach for assessing deficits in studies related to SAH, ensuring consistency across diverse laboratories and studies. Providing a multidimensional evaluation of neurological function, these systems deliver a comprehensive perspective on the impact of SAH on the nervous system (59). By utilizing objective criteria, they minimize subjectivity in assessments, enhancing result reproducibility. Additionally, these scoring systems enable researchers to track temporal changes in neurological function, offering insights into the progression and potential recovery of deficits over time. However, they may exhibit limitations, including potential insensitivity to specific deficits, interobserver variability despite objectivity, and the need for species-specific adaptations to accommodate behavioral differences among different species or strains (60).

Table. 1: Garcia Neurological Score Parameter

Score	Spontaneous Activity	Symmetry of Limb Movement	Forepaw Outstretching	Climbing	Body Proprioception	Response to Vibrissae Touch
3	Normal spontaneous activity	Normal symmetrical movement of all limbs	Normal outstretching of both forepaws	Normal climbing with good coordination	Normal proprioception, quick and coordinated response	Normal and prompt response to vibrissae stimulation
2	Decreased activity But still responsive	Slight asymmetry or weakness in limb movement	One forepaw does not outstretch fully	Impaired climbing but can ascend a vertical surface	Delayed or incomplete response to proprioceptive stimuli	Delayed or incomplete response to vibrissae stimulation
1	Minimal activity or resting, sluggish	Obvious asymmetry or partial paralysis	Both forepaws do not outstretch fully	Can only crawl but not climb	Minimal or slow response to stimuli	Minimal response or no response to vibrissae stimulation
0	No spontaneous activity	Complete paralysis or absence of limb movement	Neither forepaw outstretches fully	Unable to crawl or climb	Absence of response	Absence of any response

*Mice are observed by by an observer blinded to the experimental conditions and freely moving in an open field, and a numerical score (0-3) is assigned for six parameters, The cumulative score, obtained by summing the individual parameter scores, yields the total Garcia score for each mouse. Ranging from 3 to 18, a higher score indicates better neurological function, suggesting milder deficits, while a lower score suggests more significant impairments in mouse models.

Table. 2: Bederson Score Parameters:

Score	Circling Behavior	Forelimb Flexion	Resistance to Lateral Push
0	Normal spontaneous movement with no circling	Normal extension of both forelimbs	Normal resistance, no pushing
1	Mild circling to one side	Flexion of one forelimb	Moderate resistance to lateral push
2	Frequent circling to one side	Flexion of both forelimbs	Severe resistance, but mouse can be pushed to the side
3	Continuous circling to one side	No forelimb extension	Minimal or no resistance to lateral push

*The Bederson score is normally performed by an observer blinded to the experiment conditions. The cumulative score, ranging from 0 to 9, where higher scores signify greater impairment, and lower scores indicate milder deficits.

Table. 3: Neurological Severity Score Parameters

Score	Motor Function	Arousal and Alertness	Circling Behavior	Reflexes
0	Normal motor function	Normal arousal and alertness	No circling behavior	Both forelimb and hindlimb withdrawal reflexes present
1	Partial limb flexion	Aroused only by vigorous stimuli	Circling behavior observed	Absent forelimb or hindlimb withdrawal reflex
2	Unable to place both forelimbs	Reduced alertness, delayed response to stimuli	-	Both forelimb and hindlimb withdrawal reflexes absent
3	Unable to place the contralateral forelimb	Comatose or not aroused by any stimuli	-	-
4	Reduced spontaneous movement	-	-	-
5	Mouse moves in a circular manner when lifted by the tail	-	-	-
6	No spontaneous movement	-	-	-

*The Neurological Severity Score (NSS) ranges from 0 to 12, elevated NSS values suggest greater impairment, while lower scores indicate milder deficits. To minimize bias, it is recommended to conduct the NSS with an observer blinded to experimental conditions.

1.8.5. Autopsy Assessment of Post SAH Brain Sample

Autopsy, long considered the gold standard for evaluating SAH in mouse models, offers a comprehensive and direct examination of anatomical and histological changes post-mortem. Through precise lesion localization and quantification, histopathological assessment, and exploration of vascular anatomy, autopsy provides invaluable insights into the distribution, extent, and specific cellular alterations associated with SAH. Its role extends to identifying complications, validating model reproducibility, and contributing to a nuanced understanding of pathophysiological mechanisms. Despite its invasive nature and resource-intensive requirements, autopsy remains an indispensable tool, offering a static yet detailed snapshot critical for advancing preclinical research, enhancing our comprehension of SAH, and aiding in the development of targeted therapeutic strategies (61)(62).

Sugawara. T and colleagues (63) introduced a autopsy grading system for assessing the severity of a rodent model in the post-operative 24 hours. They utilized high-resolution images of the base of the brain, specifically focusing on the Circle of Willis and basilar arteries. In these images, the basal cistern was divided into six segments. Each segment was allotted a grade from 0–3 depending on the amount of subarachnoid blood clot in the segment as follows: Grade 0: no subarachnoid blood, 1: minimal subarachnoid blood, 2: moderate blood clot with recognizable arteries, 3: blood clot obliterating all arteries within the segment. The cumulative score, ranging from 0 to 18, where higher scores signify greater SAH severity, and lower scores indicate milder severity of SAH (Figure. 1, Table. 4).

Table. 4 Autopsy Grade Criteria

Score	Criteria
0	no subarachnoid blood
1	minimal subarachnoid blood
2	moderate blood clot with recognizable arteries
3	blood clot obliterating all arteries within the segments

*SAH: Subarachnoid Hemorrhage. Mild SAH: 0-7, Moderate SAH: 8–12, Severe SAH : 13–18.

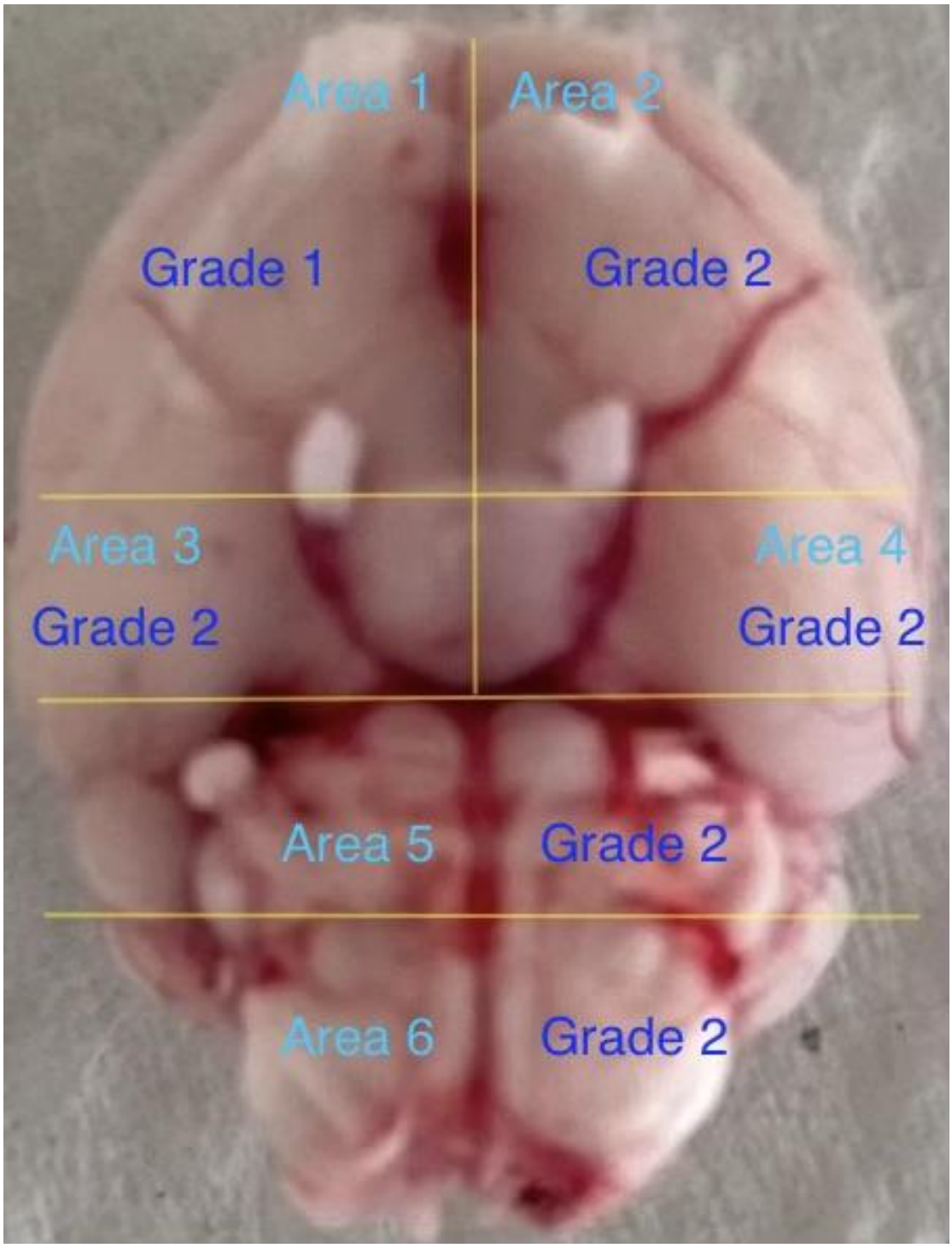

Figure. 1: Schematic Image of Autopsy Score

Fig. 1: Following the criteria established by Sugawara T et al, the ventral surface of the mouse brain was divided into six distinct areas. Each of these areas received a score ranging from 0 to 3 based on specified subarachnoid hemorrhage severity.

1.9. Aim of Study

1.9.1. Establish A Novel Surgical Approach to Induce SAH in Mouse

Among the various methodologies for inducing SAH in murine models, the classical cWp model continues to prioritize the ECA as its primary insertion site. Notably, this method necessitates sacrificing the ECA during the procedure, potentially affecting ipsilateral blood flow, pressure or even perfusion.

The intricate steps involved in this approach emphasize the need for advanced microsurgical skills, posing a steep learning curve for researchers. Recognizing the demand for a more accessible SAH modelling procedure, our study introduces a novel method. In this new approach, SAH is induced by directly puncturing the CCA and subsequently inserting the filament.

The primary objective is to simplify the technical aspects, reduce the training time, flatten the learning curve, and preserve the normal anatomical structure. This modification aims to enhance the efficiency and accessibility of preclinical SAH research methodologies.

1.9.2. Establish A Novel Post SAH Neurological Severity Assessment Score in cWp Mouse Model

A consistency in volumes of blood in subarachnoid space is important to yield comparable disease severity to include these animals for pharmacological interventions. However, it is challenging to precisely control bleeding volume during SAH induction in cWp mouse model, leading to significant post-operative variability in SAH severity among individual mice.

To address this challenge and establish a consistent starting point for preclinical SAH treatment research using the cWp mouse model, we introduce an easy-to-quantify ROB scoring system based on three objective parameters: 1). the video open field test, 2). rotarod test performance, and 3). body weight loss

measurements. Each item is assigned a different score. Based on the test results, the scores of all items are added up to get the final test score. The severity of the bleeding is then distinguished based on the total score.

2. Materials and Methods

2.1. Ethical Approval

These experiments were approved according to the guidelines of the Animal Care Committee of the District Government of North Rhine-Westphalia, Germany (Protocol Number: 81-02.04. 2021. A195).

2.2. Surgical Procedure of SAH Induction

2.2.1. Mice Cohort

A cohort of 27 male *C57BL/6* wild-type mice, aged 4 months and weighing between 25.2 to 34.9 grams, was utilized (Janvier Laboratory Le Genest-Saint-Isle, France) were used for the surgical approach establishment experiment, and another cohort of 4-month-old male *C57BL/6* mice wild type (n=40) with a body weight of around 25.3-35.5 grams were employed to establish this ROB Scoring System for assessing SAH severity, according to the guidelines of the Animal Care Committee of the District Government of North Rhine-Westphalia, Germany.

2.2.2. Perioperative Management:

Mice were fed in the human-controlled day/night rhythm, and free to food and water, before and after surgery. Standard microsurgical instruments, including 33 Gauge insulin injection needles and microsurgical forceps, were employed for the procedures. The surgical microscope provided a magnification ranging from 7 to 45 times (Leica). Anesthesia was administered to the mice, induced at 5% isoflurane and maintained at 1.5~2% isoflurane, delivered through a nose cone with 2-liter Oxygen per minute. To maintain a constant body temperature of 37.5 °C, a feedback-controlled heating pad was utilized with a setting of 37.7 °C.

2.2.3. Intraoperative ICP Monitoring and Surgical Duration

Intracranial pressure was monitored using a micro-pressure transducer from Raumedic, Germany (RAUMED Neurosmart). The sensor was positioned on the left parietal epidural space while the mice were in the prone position. After preparing the left parietal area and anesthetizing the mouse, the skull was exposed through a skin incision around 10 mm and a small burr hole around 2 mm was drilled at the parietal region. The ICP probe was then gently inserted through the burr hole into the epidural space, taking care to avoid any trauma or bleeding. Once the probe was in place, it was secured by using surgical glue, and the incision was closed. Then the mice were turned to the supine position and fixed with tape. The surgical duration was recorded from the neck incision made to the closure of this incision, excluding the ICP sensor implantation and post-SAH 15-minute observation.

2.2.4. Surgical Approach

Twelve mice underwent classical ECA approach and another twelve mice underwent modified CCA approach. Three mice underwent surgical procedure but without filament perforation as SHAM group.

ECA surgical procedure: Briefly introduce the ECA approach as described previously: the animals were anesthetized and positioned in a supine position. A midline incision was made to access the neck, and the left CCA was exposed. The ECA was tracked and dissected to its distal end as long as possible. After blocking the blood flow by micro clips or suture ligations on the artery. A 5-0 mono-filament (Prolene Ethicon) was carefully inserted through the ECA and guided into the ICA until it reached the vicinity of the anterior cerebral artery (ACA) and middle cerebral artery (MCA) bifurcation. The filament was then further advanced until a discernible and abrupt increase in ICP signified the successful induction of SAH. Subsequently, the filament was retracted into the ECA, enabling complete perfusion of the ICA (Fig. 2).

CCA surgical procedure: The exposure of the left CCA was similar as described in section of the ECA approach. However, there was no tracking and dissection of the ECA to its distal end. After a meticulous dissection of the surrounding tissue and membranes enveloping the CCA, two ligations using 5-0 silk sutures (Ethicon) were performed. The first ligation was distal, placed at the bifurcation of the ICA and ECA, while the second ligation was proximal and positioned as close as feasible to the direction of the aortic arch. Another ligation (middle ligation) was made of mono-filament dissected from the 5-0 silk suture (soft and thin) then on the segment between these two ligations near to the proximal one. CCA was punctured using 33G insulin injection needle to create an entryon the arterial wall of the CCA, precisely between the middle and proximal ligations. Care was taken to avoidback wall puncture. Subsequently, the needle was withdrawn, and a 5-0 mono-filament (Prolene Ethicon) was cautiously introduced through the puncture site. The filament was advanced along the lumen of the artery, with particular attention to preventing penetration of the back wall. Once the tip of the filament reached the location of the distal ligation, the middle ligation was tighten to fix the filament and prevent bleeding from the puncture site. The distal ligation was loosened and removed totally to create an adequate vision for the following procedure. The filament was then further advanced beyond the ICA and ECA bifurcation into the ICA. The filament was advanced tto perforate circle of Willis. Upon observing an elevation in ICP, the filament was withdrawn, with the tip repositioned back to the middle ligation before complete removal of the filament. The middle ligation was slightly tightened again but not fully closed. At this point, a controlled release of blood occurred as the filament tip exited the puncture site. The purpose of this controlled bleeding was to expel air from the arterial lumen, facilitating the formation of a blood clot at the puncture site. After short waiting period, typically less than one minute, the middle ligation could be removed, blood perfusion was reestablished via the contralateral circulation through the Willis circle. After approximately 2 to 3 minutes, the proximal ligation was gradually released, allowing observation of blood perfusion from the proximal to the distal portion of the artery and the detection of a clear arterial

pulse. Once this state was confirmed, waiting for another 2 to 3 minutes, then the proximal ligation was fully removed. Throughout this procedure, the proximal ligation could be readily re-tightened in case of excessive bleeding, providing effective control over the bleeding process (Fig. 3, Fig. 4, Fig. 5). Surgical duration and ICP value were recorded for further investigation.

2.2.5. Postoperative Rehabilitation

The incision closure was made in a routine fashion, and the mice were kept in the cage over a heating pad and wet food on the floor of the cage to facilitate reaching.

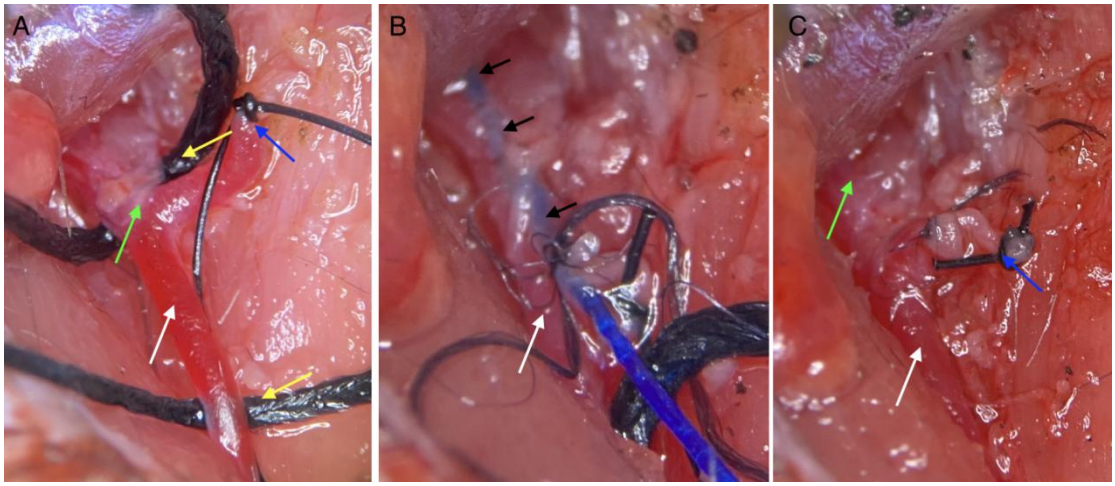

Figure. 2: Sequential Steps of the External Carotid Artery (ECA) Puncture Approach for the Circle of Willis Perforation Subarachnoid Hemorrhage Model

Fig. 2: Fig. 2A: The stump of the external carotid artery (ECA) is highlighted by the blue arrow. The ECA-internal carotid artery (ICA) bifurcation is exposed as indicated by the green arrow. Ligations (indicated by the yellow arrows) are applied to both the distal and proximal ends of the common carotid artery (CCA)(indicated by the white arrow).

Fig. 2B: Insertion of the nylon filament (indicated by the black arrows) through the ECA stump, progressing into the ICA to complete the perforation. The white arrow indicates the CCA.

Fig. 2C: The ECA approach results in sacrificing the ECA indicated by the blue arrow. And the CCA (indicated by the white arrow) and ICA (indicated by the green arrow) resume the blood flow after the removal of the ligations.

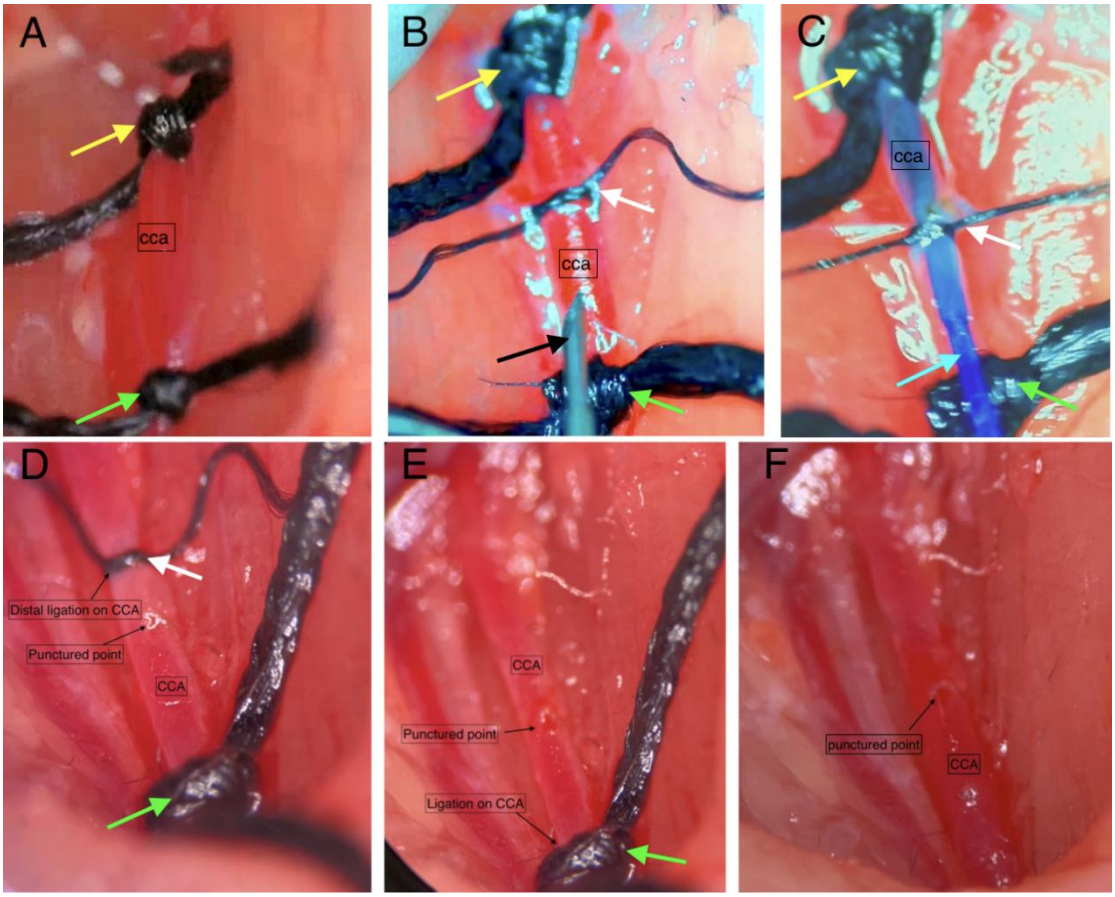

Figure. 3: Sequential Steps of the Common Carotid Artery (CCA) Puncture Approach for the Circle of Willis Perforation Subarachnoid Hemorrhage Model

Fig. 3: Fig. 3A: Isolation and Ligation: The cervical segment of the CCA is isolated, followed by proximal and distal ligation.

Fig. 3B: Puncture and Middle Ligation: A prepared middle ligation and a 33-gauge needle are used to puncture the CCA wall.

Fig. 3C: Filament Insertion and Fixation: The 5-0 Nylon mono-filament is inserted and fixed with the middle ligation. The distal ligation is then completely removed.

Fig. 3D: Controlled Bleeding: After successful perforation, the filament is withdrawn, and the middle ligation is slightly tightened to induce controlled, slight bleeding through the punctured site.

Fig. 3E: Blood Perfusion via Willis Circle: The middle ligation is removed, allowing blood perfusion from the contralateral side through the Willis circle.

Fig. 3F: After removal of the proximal ligation, the blood flow resumes to normal.

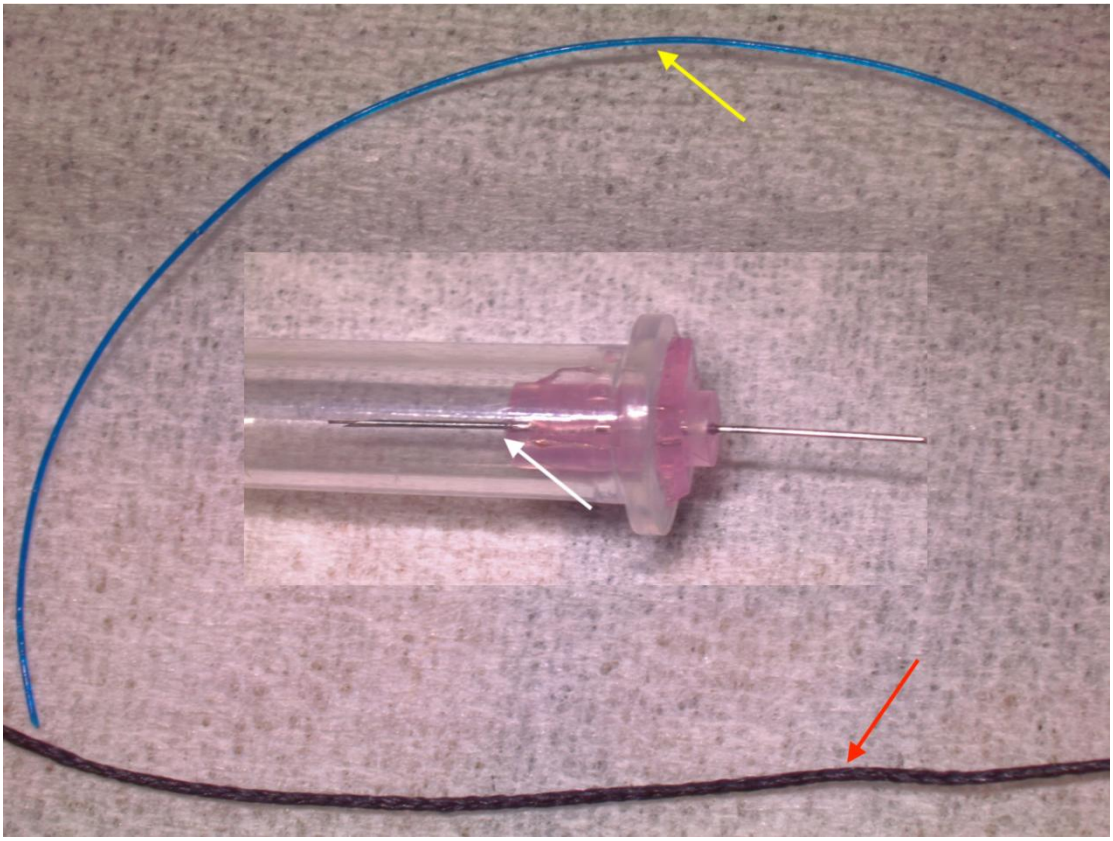

Figure. 4: Needle and Filament Applied During the Surgical Procedure

Fig. 4: The yellow arrow indicates the use of a 5-0 mono-filament (Prolene, Ethicon, USA), the red arrow indicates a 5-0 silk suture (Ethicon, USA), and the white arrow marks a 33-gauge insulin injection needle (Type C 0.2mm*4mm, TWLB, Nuofan, Ningbo, China).

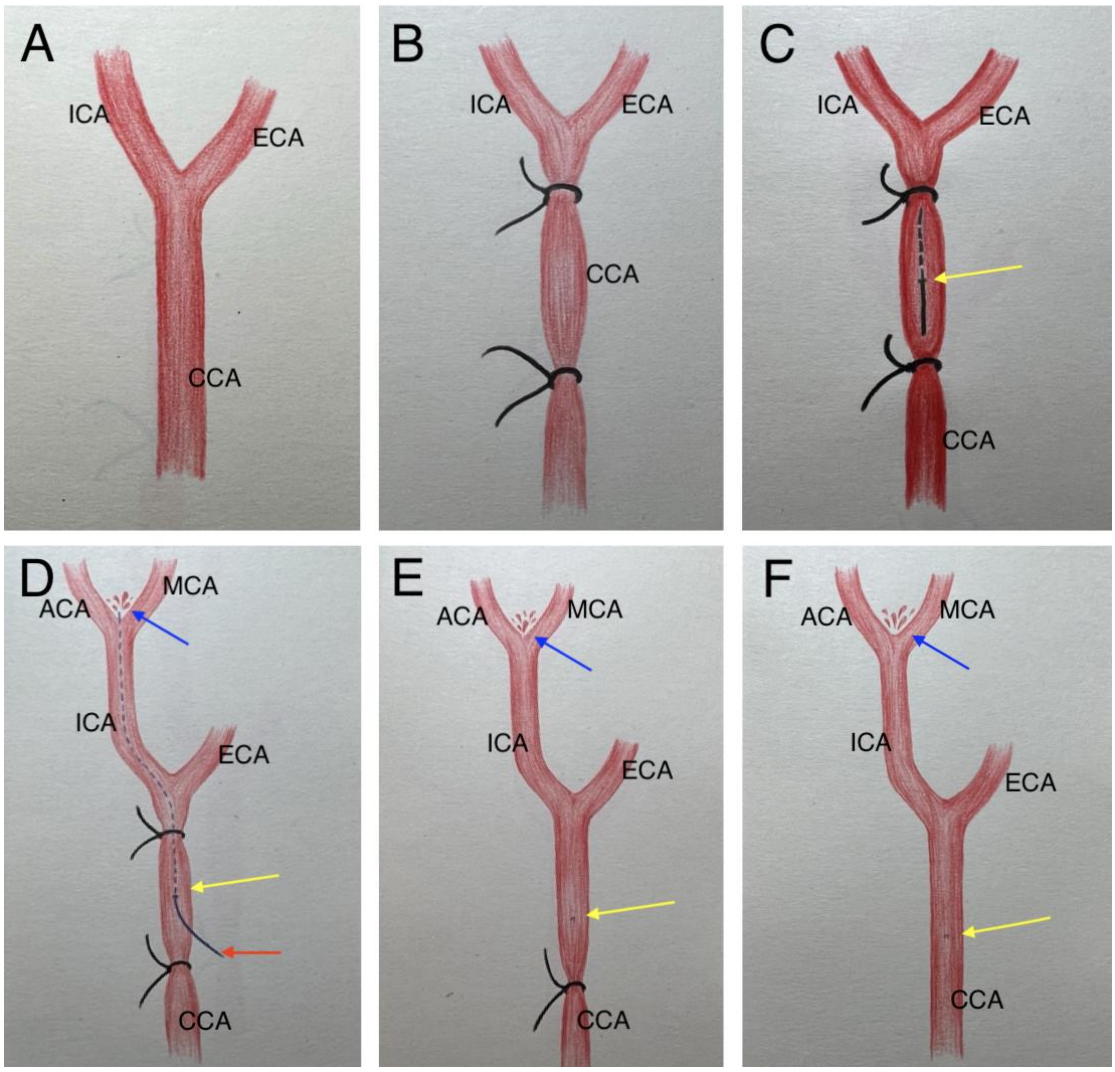

Figure. 5: Schematic of Common Carotid Artery (CCA) Approach

Fig. 5: Schematic illustrating the entire process of the CCA approach for perforating the Circle of Willis (A to F). The yellow arrow designates the puncture site on the CCA wall, while the blue arrow indicates the perforation site at the Anterior Cerebral Artery (ACA) and Middle Cerebral Artery (MCA) bifurcation. The red arrow points to the 5-0 nylon mono-filament. ICA: Internal Carotid Artery.

2.3. Post SAH Neurological Assessment

2.3.1. Rotarod Test and Body Weight Measurement

Each day, prior to conducting the Rotarod test, the body weight of the mice was measured and recorded with a precision of 0.1 grams. The body weight loss was calculated {(body weight ^{original}-body weight $^{day\ x}$)/body weight ^{original}∗100%}.

The Rotarod testing apparatus was configured in an acceleration mode, with the rotational speed ranging from 4.0 to 40 RPM (Rotation Per Minute). Subsequently, the mice were carefully positioned on the rotating rod and subjected to testing, continuing until the animal either fell from the rod to the base or the designated endpoint of 300 seconds, as stipulated by our experimental protocol (64). This testing procedure was repeated three times for each mouse, and the performance results were duly recorded. The final analysis was based on the average performance data from these three trials.

2.3.2. Video-monitoring Open Field Test

The open field test was used to analyze locomotion, anxiety and stereotypical behaviors such as grooming and rearing in rodents. The post-subarachnoid hemorrhage (SAH) mice underwent behavioral assessments in an open-field apparatus, a cubic polyvinyl chloride box measuring 42x42x42 cm (65). A 10-second video clip was recorded using a fixed-cell phone camera with parameters set to 30 frames per second (FPS). Subsequently, these video clips were subjected to analysis using the open-source software "Tracker" (version6.1) available at https://physlets.org/tracker/.

The procedure involved several sequential steps. Initially, the mouse was placed within the test field and gently immobilized at the center of the arena by securely holding its tail. Video recording was initiated, and subsequently, the mouse was released to observe its spontaneous reactions and motion. The recorded video was imported into the Tracker software. The analysis was commenced by identifying the

initial video frame where the mouse resumed its unrestricted movement. Subsequently, a specific video segment was designated for analysis, encompassing the following 160 frames, which spanned a 5-second interval. The analysis key frames were strategically positioned at five-frame intervals. The movement tracking analysis was initiated, utilizing one of the mouse's ears (either the left or right) as a tracking marker. The position of the selected ear was assessed in each key frame at the five-frame intervals.

The Tracker software automatically computed the data, including the mouse's movement trajectory and distances covered over the 5-second duration. This data was then exported and saved in Excel files to facilitate further in-depth analysis. The whole process could be completed within 2 minutes by a skilled investigator.

2.4. Criteria for ROB Scoring System

The methodology incorporated three objective parameters: rotarod test, video analysis open-field test, and daily body weight measurements. Each parameter was scored on a scale ranging from 1 to 5, contributing to a comprehensive final score within the range of 3 to 15. The ROB methodologically categorizes the post-SAH mice into three subgroups based on the disorder severity: severe (grade 3 to 6), moderate(grade 7 to 10), and mild (grade 11 to 15) (Table. 5).

2.5. Data Collection and Autopsy

For the CCA approach experiment, intraoperative intracranial pressure monitor, surgical duration, success rate, mortality, neurological assessment (including rotarod test, open-filed test, and body weight loss), and autopsy data will be collected for further research.

For the ROB score experiment, data collection occurred at specific time points: postoperative day 1, day 3, and day 7. On postoperative day 3, a subgroup of 8 mice was randomly selected for euthanasia, conducted by a researcher who was blinded to the mice's status. Brain samples from these mice were meticulously harvested and

evaluated by using the established methods(63). This evaluation entailed a comparative analysis between the ROB grade and the actual SAH status during the acute phase. The remaining mice were continually observed until day 7, at which point they were euthanized. Their findings were also compared with autopsy results to assess the sub-acute phase. The entire dataset was compiled for the purpose of comparing body weight loss, rotarod test, open field test, and mortality rates within different SAH grade groups.

Table. 5: The Criteria of ROB Score System

Score	Rotarod Test (seconds)	Open-field Test (distance)	Body Weight Loss
1	0-50	0-300	>20%
2	51-100	300-500	15-20%
3	101-200	500-800	10-15%
4	201-299	800-1000	5-10%
5	300	>1000	<5%

*Each mouse underwent daily evaluations, during which it received a performance score ranging from 1 to 5 based on its performance in individual tests. The cumulative scores from all tests were then aggregated to derive a final ROB score.

3. Results

3.1. The Outcomes of The Experiment One: Trial of Common Carotid Artery Approach

3.1.1. Workflow of CCA Approach Experiment

From the original cohort of 27 mice, three distinct groups were formed based on the type of surgery: SHAM (n=3), CCA (n=12), and ECA (n=12). Exclusions were made, specifically, two mice from the ECA group were removed due to filament insertion failure. This led to a total of 25 mice with successful surgeries considered valid for the research. Following surgery, one mouse from the CCA group died on postoperative day one, resulting in a final cohort of 24 mice, with distribution across the groups as follows: SHAM=3, CCA=11, and ECA=10. To ensure impartial evaluation, a researcher, blinded to the mice's status, randomly selected five mice from both the ECA and CCA groups. Additionally, all mice from the SHAM group underwent postoperative neurological assessment. Subsequently, all mice were euthanized, and their brains were harvested for further autopsy (Fig. 6).

3.1.2. Intraoperative Intracranial Pressure Monitoring

Both in the ECA and CCA groups, the stiff ICP elevation could be observed at the perforation success time point. The baseline in ECA and CCA were 9.5±3.0 VS 10.4±3.5 mmHg, P-Value=0.52. The ICP peak were similar to each other (ECA 51.1±12.6 VS CCA 53.5±10.6 mmHg, P-Value=0.64). And 15 minutes after the peak, the ICP dropped to 28.90±4.9 mmHg in the ECA group and 25.8±4.0 mmHg in the CCA group, the P- Value equal to 0.12 (Fig. 7, Table. 6).

3.1.3. Surgical Duration, Mortality, Success Rate, and Post SAH Neurological Assessment

The surgical duration for ECA demonstrated a notable reduction from 115 minutes to 53 minutes, indicative of improved efficiency with accumulating experience. Similarly, the CCA group exhibited a decrease from 52 minutes to 19 minutes over time. Data analysis unveiled a significant disparity between the two groups (ECA: 73±18 vs. CCA: 37±10 minutes, p-Value <0.05).

No mortality occurred during the surgical procedures, with only one postoperative day 1 death in the CCA group, resulting in a mortality rate of 8.33% (1 of 12), while the overall SAH induction mice mortality stood at 4.55% (1 of 22). Notably, the ECA group encountered filament insertion failure in 2 mice, contrasting with the CCA group where surgeries proceeded smoothly, achieving a 100% success rate in perforation.

Five mice from the ECA group, five mice from the CCA group, and three mice from the sham group underwent neurological assessments, including the Rotarod test, open-field test, and body weight monitoring. All SAH mice exhibited notable body weight loss, movement limitations, and impaired balance. In the Rotarod test, the sham group performed for 289±12 seconds, ECA for 158±67 seconds, and CCA for 122±78 seconds. Open-field test results were as follows: sham = 1156±163, ECA = 389±373, CCA = 327±224, absolute values without units were used for open field data analysis. Body weight loss percentages were recorded as sham = 1.87±0.59%, ECA = 10.08±3.44%, CCA = 10.05±2.47%. (Fig. 8, Table. 6).

3.1.4. Autopsy Outcome

The autopsy of brain samples revealed that both the ECA and CCA approaches produced a comparable spectrum of SAH severity. Further elucidation of these findings is provided in the ROB score autopsy section (Fig. 9).

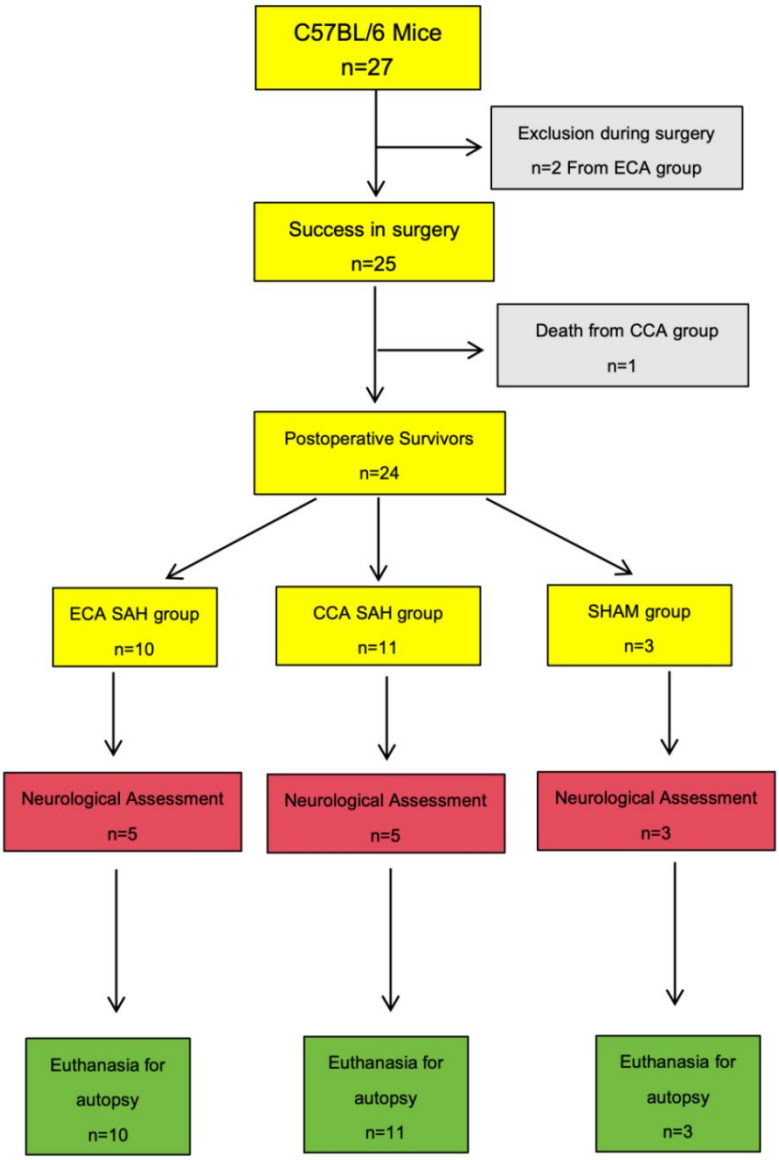

Figure. 6: Workflow of "Common Carotid Artery Approach to Establish Subarachnoid Hemorrhage Model in Mouse"

Fig. 6: Experimental plan comparing currently existing model (ECA group) to compare newly established model (CCA group). The cohort was subdivided into SHAM (n=3), ECA group (n=12), and CCA group (n=12). Two mice in the ECA group were excluded due to filament insertion failure. One mouse died from CCA group on the postoperative day one.

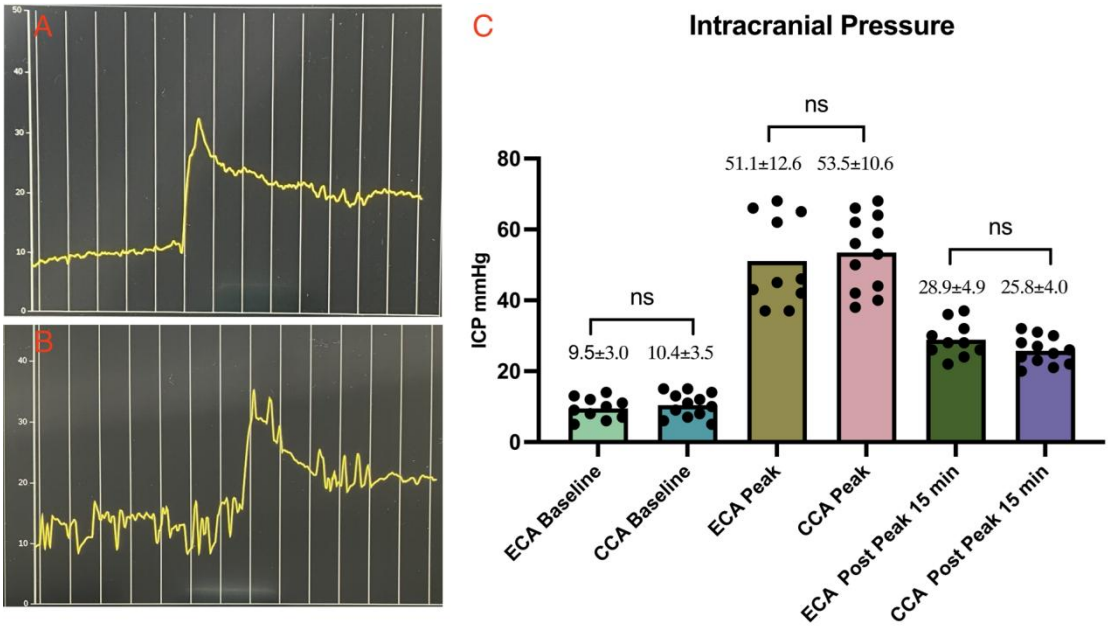

Figure. 7: Classical Schematic of Intraoperative Intracranial Pressure Monitoring and Data Comparison

Fig. 7: Figure 7A illustrates the intraoperative ICP fluctuation record in the ECA group, and Figure 7B depicts a similar fluctuation for the CCA group. Both groups exhibited the characteristic curve of ICP elevation after induction of SAH. Figure 7C: One-way ANOVA analysis revealed no significant differences in ICP baseline values, peak values, and post-peak 15-minute values in the ECA and CCA groups.

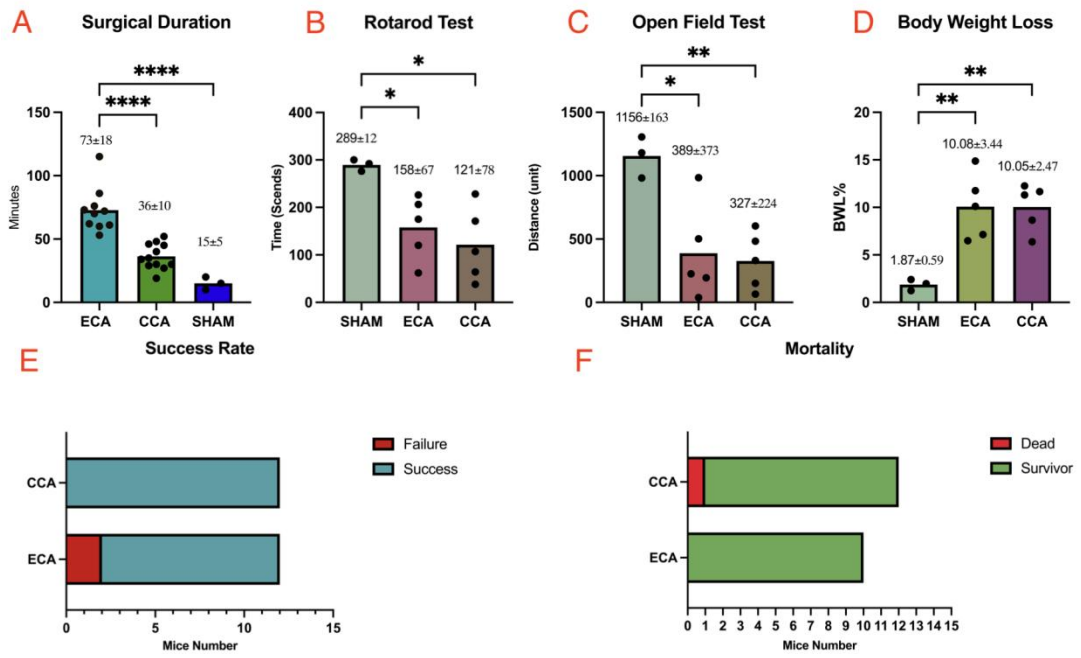

Figure. 8: Surgical Duration, Mortality, Success Rate, and Postoperative Neurological Assessment Comparison

Fig. 8: Fig. 8A Comparison of surgical duration reveals a significantly longer procedure in the ECA group compared to the CCA group ($P<0.05$). The CCA group duration is not significantly different from the Sham group, highlighting the efficient performance of the CCA approach.

Fig. 8B, 8C, 8D: Postoperative neurological assessment using the Rotarod test, open-field test, and body weight loss measurement. Both ECA and CCA SAH mice (n=5) exhibit a significant decrease in performance compared to the SHAM group (n=3) in the Rotarod and open-field tests ($P<0.05$). Body weight loss in both ECA and CCA groups is significantly higher than in the SHAM group ($P<0.05$). However, there is no significant difference between ECA and CCA groups in these parameters.

Fig. 8E: In the ECA group, two mice experienced filament insertion failure into the ICA, while all of the mice in the CCA group succeed in SAH induction.

Fig. 8F: One mouse in the CCA group died on the postoperative day one. No deaths occurred in the ECA group.

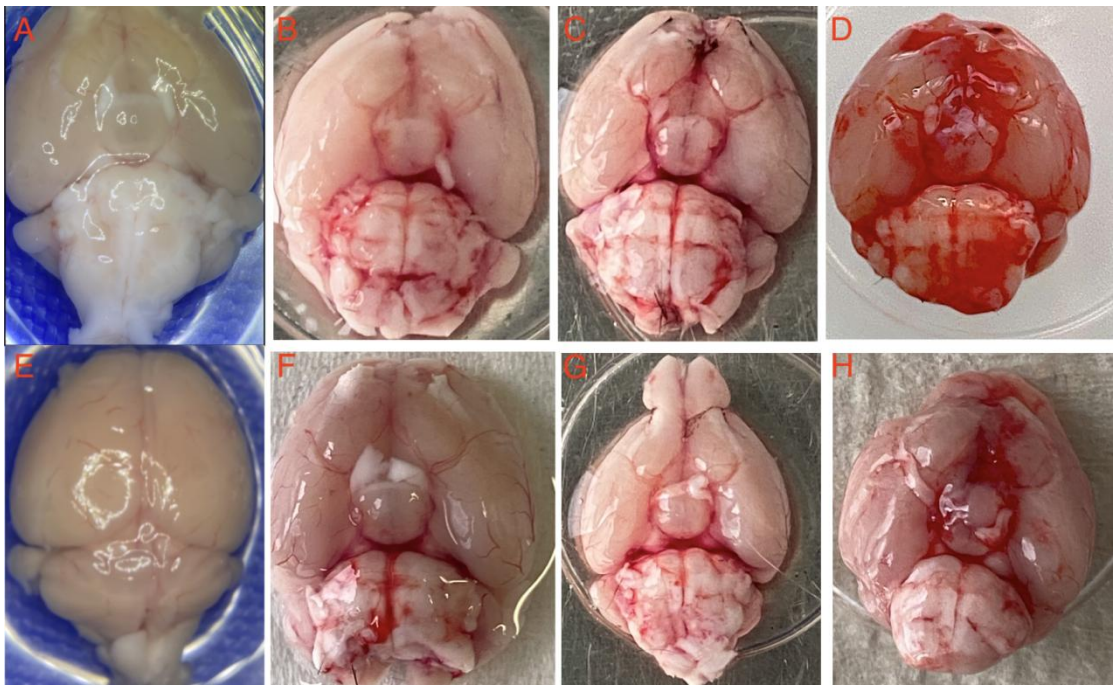

Figure. 9: Comparative Evaluation of Subarachnoid Hemorrhage Severity in the Circle of Willis Perforation Mouse Model

Fig. 9: Fig. 9A: Ventral Surface of SHAM Mouse Brain: devoid of any hemorrhage.

Fig. 9B to D - ECA Group:

B: Mild SAH

C: Moderate SAH

D: Severe SAH

Fig. 9E: Dorsal Surface of SHAM Mouse Brain: devoid of any hemorrhage.

Fig. 9F to H - CCA Group:

F: Mild SAH

G: Moderate SAH

H: Severe SAH

Images depicting different grades of SAH severity within the ECA and CCA group in the cWp mouse model.

Table. 6: Summary of Results - Intraoperative Intracranial Pressure Monitoring, Surgical Duration, Postoperative Mortality, Success Rate, and Neurological Assessment

Group	CCA	ECA	SHAM
ICP Baseline (mmHg)	10.4±3.5 n=12	9.5±3.0 n=10	--
ICP Peak (mmHg)	53.5±10.6 n=12	51.1±12.6 n=10	--
ICP 15 minutes post peak (mmHg)	25.8±4.0 n=12	28.9±4.9 n=10	--
Surgical Duration (min)	37±10 n=12	73±18 n=10	15±5 n=3
Postoperative Mortality (%)	8.33	0	0
Success Rate (%)	100	83.33	--
Postoperative Rotarod Test (seconds)	122±78 n=5	158±67 n=5	289±12 n=3
Postoperative Open-field Test	327±224 n=5	389±373 n=5	1156±163 n=3
Postoperative Body Weight Loss (%)	10.05±2.47 n=5	10.08±3.44 n=5	1.87±0.59 n=3

* One mouse from the CCA died on the postoperative day one, its intraoperative data is still valid.

The open field data analysis employed absolute values without units.

3.2. The Outcomes of The Experiment Two: ROB Score for Post Subarachnoid Hemorrhage Severity Assessment

3.2.1. Mice cohort, ROB Score Evaluation, and Group Classification

From the original cohort of 40 mice, exclusions were made as follows: one mouse was removed from the study due to an unexpected neck tumor, one mouse died during the surgical procedure due to the rupture of ICA, two mice the filament insertion was not optimal. These exclusions resulted in a total of 36 mice considered valid for the research. Subsequently, four mice were excluded due to death or euthanasia within the first 24 h that can not get their first ROB score. And three mice had missing data for postoperative day one due to the Rotarod testing machine fault. The remaining 29 mice, post ROB grading, exhibited a spectrum of scores, ranging from 4 to 13. This variation led to the categorization of six mice into the severe SAH group, eighteen into the moderate SAH group, and five into the mild SAH group based on the severity of their condition on the postoperative day one (Fig. 10).

3.2.2. Mortality

The intraoperative and first 24-hour mortality in the SAH induction group was 13.51% (5 of 37 mice). Which is slightly lower to the our previous meta-review paper reported (66). The overall mortality rates of the valid 29 mice at different time points were as follows: 0% (0 of 29) on Day 1, 10.34% (3 of 29) on Day 2, 13.79% (4 of 29) on Day 3, 38.1% (8 of 21) at Day 4, and 38.1% (8 of 21) on day 7. Notably, the severe group exhibited an overall mortality rate of 66.67% (4 of 6) on day 3 and 100% (6 of 6) on day 4. In contrast, the moderate and mild groups experienced no mortality on day 3. On postoperative day 7, the mortality rate for the moderate group was 15.38% (2 of 13), while the mild group continued to show no death. The final survivors came from moderate and mild groups, with no mice from the severe group, based on the postoperative day one evaluation. Thus mortality comparison made and analyzed by

survival log-rank test showed a significant difference between those groups, P<0.001 (Table. 7, Fig. 11).

3.2.3. Autopsy Results on Day Three and Day Seven

According to the autopsy scoring system (Fig. 1, Table. 4), eight mice underwent euthanasia on day 3. The autopsy examinations exhibited close alignment with the assigned Day 3 ROB grades. Among the randomly chosen subset of five mice, four received similar scores (Table. 8, Fig. 12). On day 7, a parallel congruence was evident among four randomly selected mice from a total of thirteen. In three of four mice, similar scores were observed, providing affirmation of the correlation between the assigned ROB grades and autopsy examinations (Table. 9, Fig. 13).

3.2.4. Neurological Assessment Outcomes on Postoperative Day One

We systematically recorded and conducted a comparative analysis of individual parameters within each group. The result of Rotarod test in groups (unit: seconds): Overall (n = 29): Range = 0-215, Mean ± SD = 106 ± 68; Severe (n = 6): Range = 0-154, Mean ± SD = 38 ± 60; Moderate (n = 18): Range = 0-177, Mean ± SD = 106 ± 51; Mild (n = 5): Range = 151-215, Mean ± SD = 188 ± 30. The result of Open-field test in groups (Distance, absolute value without unit): Overall (n = 29): Range = 39-944, Mean ± SD = 402 ± 266; Severe (n = 6): Range = 39-277, Mean ± SD = 130 ± 92; Moderate (n = 18): Range = 90-944, Mean ± SD = 425 ± 251; Mild (n = 5): Range = 492-891, Mean ± SD = 643 ± 169. The result of Body Weight Loss in groups (Percentage %): Overall (n = 29): Range = 1.57-16.23, Mean ± SD = 8.29±4.78; Severe (n = 6): Range = 3.21-16.23, Mean ± SD = 11.00±5.36; Moderate (n = 18): Range = 2.73-14.89, Mean ± SD = 9.07 ± 3.87; Mild (n = 5): Range = 1.57-4.00, Mean ± SD = 2.23 ± 1.00. The obtained results were meticulously documented (Table. 7, Fig. 11, Fig. 14).

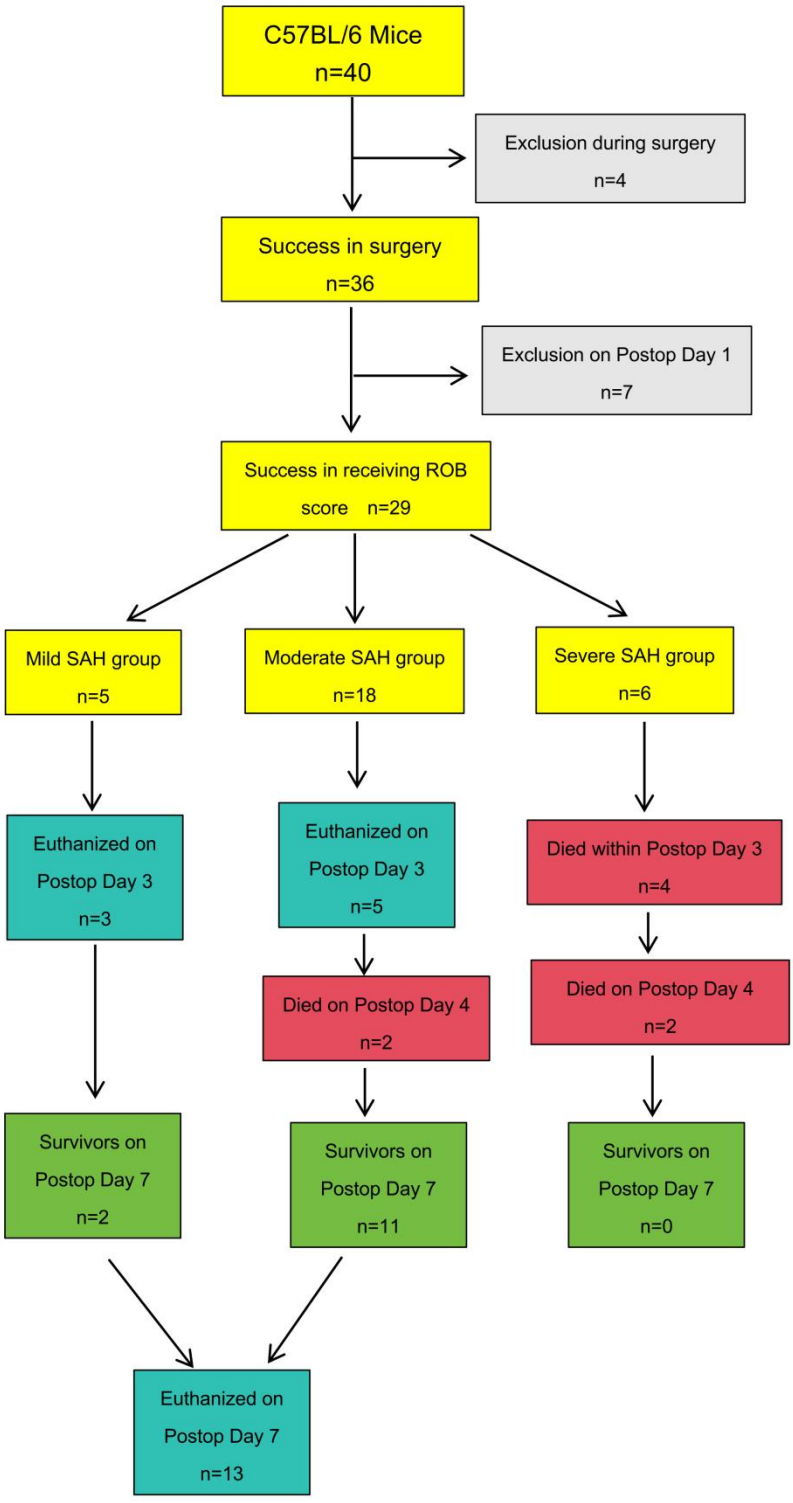

Figure. 10: Workflow of The ROB Score Experiment

Fig.10: Workflow of ROB experiment. Exclusion were made intra- and post-operative. Eight mice were randomly chosen and euthanized on postoperative day 3. The survivors on postoperative day 7 were all euthanized (Postop: Postoperative).

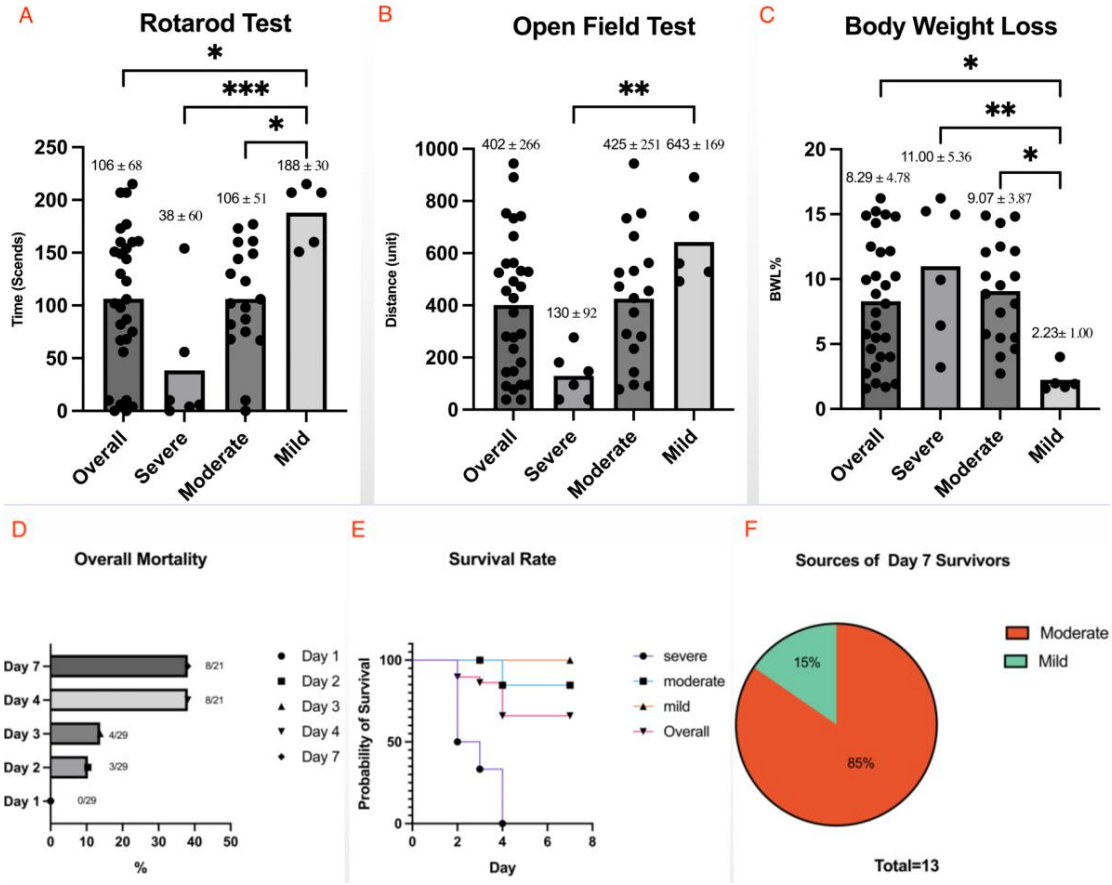

Figure. 11: Comparative Analysis of Postoperative Neurological Performance Metrics Across Experimental Groups

Fig. 11: Fig. 11A: Rotarod Test Results: Utilizing ordinary one-way ANOVA multiple comparisons, significant differences ($P < 0.05$) were observed between overall performance and mild outcomes, severe and mild outcomes, as well as moderate and mild outcomes. However, no significant differences were detected in the comparisons between overall and severe, overall and moderate, and severe and moderate groups.

Fig. 11B: Open-Field Test Results: Significance ($P < 0.05$) was found only in the severe vs. mild comparison, while other pairings did not exhibit statistical significance.

Fig. 11C: Body Weight Loss: Consistent with Rotarod results, three comparisons (overall vs. severe, overall vs. moderate, and severe vs. moderate) showed no

significant differences, while the remaining three comparisons (overall vs. mild, severe vs. mild, and moderate vs. mild) revealed significant differences ($P < 0.05$).

Fig. 11D: Mortality Trends: The mortality of 29 post-SAH mice increased over time. Notably, on postoperative day 3, eight mice were randomly euthanized, and the total number of mice overall was reduced to 21.

Fig. 11E: Survival Rate Comparison: Survivor log-rank analysis demonstrated a significant difference ($P < 0.0001$) in survival rates among the groups.

Fig. 11F: Post-operative Day 7 Survivor source: Thirteen mice survived on postoperative Day 7, 2 from mild, and 11 from moderate, with no survivors in the severe group.

Table. 7: The Postoperative Results of Mortality, Rotarod Test, Open-field Test, and Body Weight Loss in Each Group

Group	Mortality (%)(D3)	Mortality (%)(D7)	Rotarod Test (seconds)(D1)		Open-field Test (D1)		Body Weight Loss (%) (D1)	
Overall n = 29	13.79	38.1	Range	0-215	Range	39-944	Range	1.57-16.23
			Mean ± SD	106 ± 68	Mean ± SD	402 ± 266	Mean ± SD	8.29±4.78
Severe n = 6	66.67	100	Range	0-154	Range	39-277	Range	3.21-16.23
			Mean ± SD	38 ± 60	Mean ± SD	130 ± 92	Mean ± SD	11.00±5.36
Moderate n = 18	0	15.38	Range	0-177	Range	90-944	Range	2.73-14.89
			Mean ± SD	106 ± 51	Mean ± SD	425 ± 251	Mean ± SD	9.07 ± 3.87
Mild n = 5	0	0	Range	151-215	Range	492-891	Range	1.57-4.00
			Mean ± SD	188 ± 30	Mean ± SD	643 ± 169	Mean ± SD	2.23 ± 1.00

*Unit: Open-field test: distance (absolute value without unit). D1: Postoperative Day one. D7: Postoperative Day seven.

Figure. 12: Original Image of Brain Sample on Postoperative Day Three

Fig. 12: Illustrates the original images of five randomly selected mice from a cohort of eight euthanized specimens. The variance observed in subarachnoid hemorrhage (SAH) levels on Postoperative Day 3 is assessed through an autopsy score.

Table. 8: Post-operative Day Three Comparison Between Autopsy Score and ROB Score

Animal ID	T8	T9	T11	T12	T13
Autopsy Area 1	2	1	2	0	1
Autopsy Area 2	1	0	1	0	1
Autopsy Area 3	2	2	3	2	1
Autopsy Area 4	2	2	3	2	2
Autopsy Area 5	2	1	2	2	2
Autopsy Area 6	2	1	2	1	2
Autopsy score	11	7	13	7	9
ROB score	10	14	8	11	10
Autopsy severity	moderate	mild	severe	mild	moderate
ROB severity	moderate	mild	moderate	mild	moderate

*Autopsy on the postoperative day 3 revealed the high correlational signs between the autopsy score and ROB score.

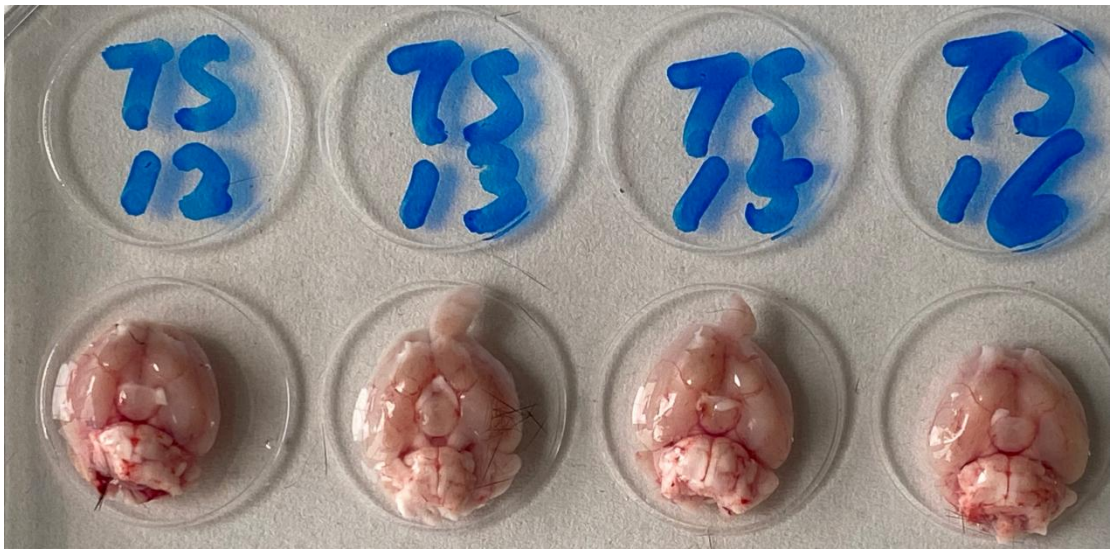

Figure. 13: Original Image of Brain Sample on Postoperative Day Seven

Fig. 13: Illustrates the original images of four randomly selected mice from a cohort of thirteen euthanized specimens. The variance observed in subarachnoid hemorrhage (SAH) levels on Postoperative Day 3 is assessed through an autopsy score.

Table 9: Postoperative Day Seven Comparison Between Autopsy Score and ROB Score

Animal ID	TS12	TS13	TS15	TS16
Autopsy Area 1	0	1	0	0
Autopsy Area 2	0	0	0	0
Autopsy Area 3	2	0	2	2
Autopsy Area 4	2	0	2	2
Autopsy Area 5	1	1	1	1
Autopsy Area 6	1	0	0	1
Autopsy Score	6	2	5	6
ROB score	12	8	14	12
Autopsy severity	mild	mild	mild	mild
ROB severity	mild	moderate	mild	mild

*Autopsy on the postoperative day 7 revealed the high correlational signs between the autopsy score and ROB score.

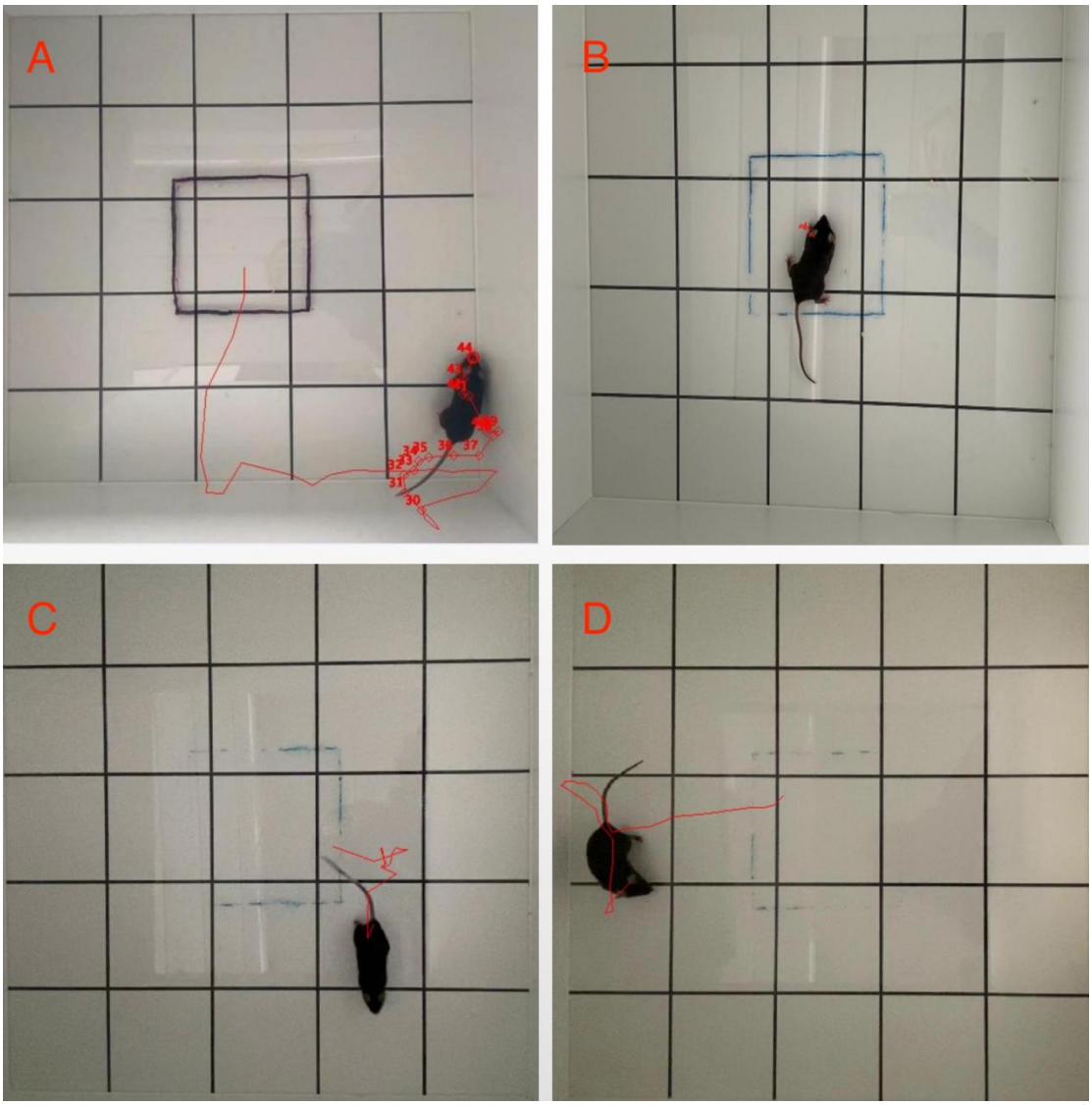

Figure. 14: Trajectory Analysis of Mouse Movement in The Open-field Test

Fig. 14: In this figure, the video analysis software "Tracker" was utilized to automatically analyze and generate trajectories illustrating the movement patterns of mice in the arena. The red line represents the tracked movement distances for mice in different conditions. Fig. 14A: Depicts a sham mouse exhibiting swift and positive movement during the testing process. Fig. 14B: Illustrates a mouse in a severe condition, displaying minimal movement and almost a frozen state throughout the testing process. Fig. 14C: Illustrates a moderate mouse movement, covering approximately half the distance compared to the sham mouse. Fig. 14D: Shows a mild status mouse movement, which closely resembles the movement pattern of the sham mouse.

4. Discussion and Conclusion

4.1. Aneurysmal Subarachnoid Hemorrhage Preclinical Research

The etiology of subarachnoid hemorrhage (SAH) is diverse, encompassing traumatic, aneurysmal, or arteriovenous malformation (AVM)-related causes, along with instances where the exact cause remains unclear (67). Among these, the rupture of intracranial aneurysms stands out as the most prevalent and consequential factor leading to SAH (2).

Aneurysmal subarachnoid hemorrhage (aSAH) represents a critical clinical emergency marked by its acute onset, demanding immediate attention due to substantial mortality rates. The acute phase of aSAH carries an inherent risk, with mortality rates varying based on the severity of the initial bleed and the emergence of complications such as early brain injury. Studies have reported acute mortality rates ranging from 10% to 50%, highlighting the urgency and gravity of this phase (5)(6)(7). Transitioning into the chronic phase, aSAH continues to exert a significant toll on patients. Chronic mortality rates, often reported up to a year post-event, Roquer, J., et al reported in 2020, the 5-year mortality of aSAH was 29% although the patients were treated with the current guidelines (68). However, the aftermath of aSAH extends beyond mortality concerns, encompassing a spectrum of post-SAH complications (8). Cerebral vasospasm (CVS), a vasoconstrictive phenomenon, poses a persistent threat to patients, contributing to delayed cerebral ischemia and further complicating the recovery process. Additionally, DIND/DCI emerges as a formidable challenge, reflecting the intricate interplay of various pathophysiological mechanisms. Hydrocephalus, another common sequelae, adds to the complexity of post-SAH scenarios, necessitating vigilant monitoring and intervention. Cognitive impairment, often underreported but significant, further shapes the long-term quality of life for survivors (16)(69)(70).

In spite of advances in medical science, SAH continues to be associated with poor outcomes. This lingering challenge can be attributed to the intricate and multifaceted mechanisms underlying SAH pathology. Despite decades of research, clinical physicians and scientists still grapple with a limited understanding of these complex processes, impeding the development of targeted interventions to improve prognosis (68). The elusive nature of SAH outcomes underscores the pressing need for further investigation and a concerted effort to expand our knowledge base.

In the realm of aSAH preclinical research, animal models, particularly the mouse model, have become indispensable tools. The mouse model offers several advantages that enhance its utility in studying SAH pathophysiology and potential therapeutic interventions. Mice are cost-effective, have a short reproductive cycle, and facilitate gene modification, enabling the exploration of specific molecular mechanisms (39)(40). Furthermore, their amenability to large-scale experimentation makes them an ideal choice for robust preclinical studies. The versatility of the mouse model positions it as a cornerstone in advancing our understanding of aSAH and holds promise for uncovering novel therapeutic avenues to enhance patient prognosis (71).

4.2. Circle Willis Perforation Mouse Model and Its Novel Protocol of Establishment

The cWp model represents a modification derived from the Middle Cerebral Artery Occlusion (MCAO) model (72), which was first reported by Kamii, H. et al in 1999 (38). It has emerged as the most representative choice in SAH research due to its unparalleled advantages, closely mirroring the natural progression of the human disease. This model excels in faithfully replicating the entire spectrum of SAH processes—from the initial vessel rupture and bleeding into the subarachnoid space to the subsequent elevation of intracranial pressure, reduction in cerebral blood flow, and the rapid onset of vascular vasospasm. Importantly, the cWp mouse model extends its utility beyond the acute phase, faithfully recapitulating post-SAH events

such as inflammation and delayed ischemic neurological deficits. This remarkable fidelity to the complex pathophysiology of SAH positions the cWp mouse model as an indispensable and optimal tool for preclinical research in this field, offering invaluable insights that can significantly contribute to advancing our understanding and therapeutic approaches for this challenging condition (38)(39)(73)(74).

While several modified versions of the cWp model have been proposed, the classical cWp model still retains the ECA as its primary insertion site (75). It's remarkable to note that in this approach, the ECA must be sacrificed during the procedure, which may affect the hemodynamic changes, cerebral perfusion and shear stress in vascular wall impacting the post SAH pathophysiological mechanisms (76)(77).

Simultaneously, it's worth noting that in the classical cWp model, where the ECA is the chosen insertion site, the ECA itself needs to be dissected along the artery in its distal direction to create as much space as possible. This step is crucial for facilitating subsequent manipulations and ensuring the accuracy and effectiveness of the procedure. In some cases, the authors have also opted to sacrifice the Pterygopalatine artery (39). These complex manipulations underscore the demand for experienced microsurgical skills, as executing such intricate steps can present a challenging cliffy learning curve for researchers leading to a huge impact on the reproducibility of the experiment.

Simplifying the SAH modeling procedure is of paramount importance to enhance reproducibility and reduce confounders in preclinical SAH research. In this study, we introduced a novel method for inducing SAH by directly puncturing the CCA and subsequently inserting the filament building upon the Seldinger technique (78). This approach aims to streamline the technical complexities and improve the learning curve associated with the procedure (Fig. 3, Fig. 4, Fig.5, video. 1).

Surgical procedures were conducted to assess the feasibility of the novel CCA approach, with a comparative analysis against the conventional ECA approach. A

proficient neurosurgeon conducted surgeries using standard microsurgical instruments, a 5-0 Nylon filament, and a 33-gauge needle via the CCA approach. Additionally, the ECA approach was performed following the protocol described in a prior study (39). The study cohort was subsequently categorized into three groups based on the type of surgery: SHAM (n=3), ECA (n=12), and CCA (n=12) (Fig. 2, Fig. 3, Fig. 4, Fig. 5, Fig. 6).

Upon evaluating various outcomes, including intracranial pressure fluctuation, mortality, success rates, and postoperative neurological assessments in the SAH model, we found no discernible differences between the two surgical routes. Moreover, SAH induction in the CCA group yielded comparable results to the ECA group during autopsy examinations. A striking observation was the significantly reduced surgical duration in the CCA puncture group, underlining the efficiency of this novel method (Fig. 7, Fig. 8, Fig. 9, Table. 6).

4.3. ROB Score and Its Ability to Distinguish The Severity of SAH in Mice

In preclinical SAH research cWp model and cisterna Magna blood injection models provide excellent tools. However, with few strengths and weaknesses of both models that need to be addressed during preclinical pharmacological interventional studies.

Cisterna Magna blood injection model provide generate a consistent blood volume in the subarachnoid space via controlled injection of particular blood volume but the model does not really mimic the clinical SAH pouring blood from arterial/aneurysm rupture. The cWp model on the other hand provide more resemblance with clinical SAH pouring arterial blood in the subarachnoid space with heterogeneity in blood volume producing different grades of severity very similar to the clinical situation. For investigations focusing on pathophysiological mechanisms of disease, particularly mechanisms in the EBI phase, cWp model is the most suitable

currently available model. However, for preclinical pharmacological interventions using cWp model, the disease severity may add bias. Hence, to address this aspect disease severity score and analyzed mortality in different groups. The application of newly developed score provides valuable tool to find mechanisms underlying SAH and offers a platform for the development of potential therapeutic interventions. Again, the choice of the SAH model is a critical consideration, and the cWp model emerges as a strong contender due to its ability to closely mimic the natural disease process observed in humans. This model offers a bridge between experimental research and clinical relevance. Nevertheless, it is crucial to acknowledge the limitations inherent in the cWp model, particularly the considerable variability in post-operative outcomes among individual mice. This heterogeneity poses a challenge in translating findings to the clinical setting and underlines the importance of refining and standardizing this model (62)(79)(80).

Evaluating the neurological deficits in SAH mice is a fundamental aspect of experimental design. Various protocols have been established to assess post-SAH neurological outcomes. However, some of these protocols rely on subjective assessments by observers, introducing potential bias and inter-observer variability. Subjective evaluation can be influenced by individual interpretation and experience, which may impact the reliability of the results (56).

Moreover, certain assessment protocols necessitate the euthanasia of animals and subsequent autopsy to define the severity of neurological deficits. While such approaches may yield valuable data, they are inherently invasive and limit the ability to monitor long-term recovery (63)(81).

Certainly, much like in human medicine, computer tomography (CT) and magnetic resonance imaging (MRI) are powerful tools for investigating the severity of SAH in mouse models. However, it's important to acknowledge that these imaging modalities come with certain practical limitations. The equipment itself can be costly, and conducting CT or MRI checks in mouse models may not always be convenient due to various factors, including availability, logistics, and the small size of the

animals (82)(83)(84). Therefore, it becomes imperative for researchers to consider and develop more objective, non-invasive assessment methods that minimize observer bias and support longitudinal monitoring.

In the clinical context, grading systems like the Hunt & Hess Scale (85) or Glasgow Coma Scale (GCS) (86) have long served as valuable tools to evaluate and categorize the severity of SAH in human patients. Inspired by Hunt & Hess scale and GCS, we introduced a novel grading system known as the ROB score, including rotarod tests, open field tests, and body weight loss.

When comparing the results of the ROB categorization with the autopsy grading results, satisfactory alignment was observed. On postoperative day 3, 4 out of 5 randomly selected samples exhibited concordant results with the autopsy findings. Similarly, on postoperative day 7, 3 out of 4 randomly chosen samples demonstrated congruent outcomes, particularly in recognizing the resorption of the bleeding. It is noteworthy that this observed bias is within an acceptable range both in the acute and sub-acute phases of SAH, however, in the chronic phase, the ROB score will be more accurate than the autopsy score due to the DIND/DCI (Fig.2).

Indeed, our study employing the ROB score to categorize the severity of SAH in mouse models revealed an interesting observation. The ROB score successfully divided the SAH mice into three subgroups based on severity, the mortality in subgroups demonstrated an obvious bias, meanwhile, the post-operative status of these mice couldn't be accurately represented by any single parameter (RT, OT, and BWL). For instance, when considering body weight loss, there was no significant difference between the severe and moderate groups (11.00% ± 5.36% vs. 9.07% ± 3.87%, p-value = 0.7877). A similar lack of significance was observed in RT and OT. However, it's crucial to note that postoperative mortality exhibited substantial deviations (P value <0.0001) among these groups, with stark differences observed on Day 3 (66.67% vs. 0%) and Day 7 (100% vs. 15.38%) (Fig. 1). This observation underscores the added value of the ROB score in providing a comprehensive and

nuanced assessment, consolidating multiple parameters into a single, informative metric for precise categorization of SAH severity (Fig. 1).

The introduction of the ROB system represents a significant advancement in the field of SAH research to accurately allocate mice with different disease severity in control and interventional groups providing accurate data on the efficacy of tested drugs Here are a few aspects of our SAH severity score that will certainly enhance the quality of preclinical SAH research.

4.3.1. Precise Classification of SAH Severity

The ROB grading system excels in its ability to precisely classify SAH models into three distinct subgroups: severe, moderate, and mild. This refined categorization of SAH severity is essential to our study as it enables us to differentiate the data within each subgroup. For instance, on postoperative Day 3, the overall mortality rate stands at 13.79%. However, within the severe group, this rate soars to 66.67%, representing nearly fivefold higher mortality. This striking disparity highlights a fundamental insight – a simplistic division of experimental subjects into "sham" and "SAH" groups falls short of capturing the complexity of the condition. A more detailed classification is imperative. In practice, dichotomous categorization of "sham" and "SAH" would disregard the inherent diversity in SAH severity, potentially leading to misleading or inconclusive findings, especially in the drug treatment trial. So this precision in classification results in a more comprehensive understanding of SAH and its outcomes, ultimately elevating the quality and relevance of our research.

4.3.2. Dynamic Evaluation and Timely Identification

The ROB grading system not only provides a static assessment of SAH severity but also offers dynamic evaluation. The ability to assess and update the ROB grade every day after the surgery is invaluable. This dynamic assessment aids in the prediction of adverse outcomes, including the death of mice. By recognizing the ROB

grade as a predictive tool for identifying severe cases, our research contributes to the advancement of animal welfare. This early identification and intervention can mitigate suffering and improve the ethical treatment of research animals.

4.3.3. Promoting Uniformity in Experimental Models

By offering an accurate and refined method for identifying the severity of SAH, the ROB grading system serves as a transformative tool in making the cWp mouse model closely resemble the injection model. This alignment represents a substantial stride towards providing a standardized and uniform experimental model for various applications. The practical implications of this uniformity are profound. In drug treatment studies, for instance, exclusion of severe or mild could be possible, the uniform cWp mouse model ensures that experimental outcomes are less influenced by variations in disease severity. This reliability in experimental conditions enhances the validity of findings and strengthens the foundation for potential therapeutic interventions.

4.4. Conclusion and Limitation

4.4.1. The Novel CCA Surgical Approach for cWp Mouse Modelling

In summary, the CCA approach offers two eminent advantages in the context of SAH modeling. Firstly, it simplifies surgical manipulation, leading to significantly shorter surgical duration. Secondly, it preserves the integrity of all anatomical structures, eliminating the need for complex artery dissections. Crucially, our research has demonstrated that the CCA approach can generate a SAH model of the same quality as the ECA approach while reducing confounders and time of surgical procedure as well as the time for anesthesia. This underscores the potential of the CCA approach to serve as a streamlined and equally reliable alternative for SAH mouse model production, reducing surgical complexity while maintaining research rigor.

As a novel surgical approach, the sample scale in our study is limited, the further investigation is still demanded in its application, Feedback from other researchers is valuable to make this approach perfect. In summary, our efficient protocol provides a high-quality SAH model in mice while preserving normal vascular structures. This approach should be considered for widespread adoption in SAH research.

4.4.2. ROB Score System

The perforation SAH mouse model plus ROB score could meet this demand: (1) reproducible and consistent blood deposition in the subarachnoid space, (2) uniform, controlled degree of hemorrhage,(3) mechanism of hemorrhage closely simulating aneurysmal SAH,(4) blood distribution correlating with aneurysmal SAH,(5) ease to performance and (6) reasonable costs (87).

However, being a novel protocol, it is essential to acknowledge the inherent limitations of our study. The sample size in our experiment is relatively small, and we recognize the necessity for the SAH translational research community to adopt and further validate our protocol in their investigations. As the sample size increases in future studies, it may be prudent to consider adjustments to the criteria of the ROB for enhanced robustness and generalizability.

5. References

1. Terpolilli NA, Brem C, Buhler D, Plesnila N. Are We Barking Up the Wrong Vessels? Cerebral Microcirculation After Subarachnoid Hemorrhage. Stroke. 2015;46(10):3014-9.

2. Wiseman JE, Agange N, Milliken JC. Coarctation of the aorta presenting as spontaneous subarachnoid haemorrhage in the absence of cerebral aneurysm: a report of a rare clinical entity. Heart Lung Circ. 2010;19(7):432-4.

3. Ingall T, Asplund K, Mahonen M, Bonita R. A multinational comparison of subarachnoid hemorrhage epidemiology in the WHO MONICA stroke study. Stroke. 2000;31(5):1054-61.

4. de Rooij NK, Linn FH, van der Plas JA, Algra A, Rinkel GJ. Incidence of subarachnoid haemorrhage: a systematic review with emphasis on region, age, gender and time trends. J Neurol Neurosurg Psychiatry. 2007;78(12):1365-72.

5. Long B, Koyfman A, Runyon MS. Subarachnoid Hemorrhage: Updates in Diagnosis and Management. Emerg Med Clin North Am. 2017;35(4):803-24.

6. Behrouz R, Sullebarger JT, Malek AR. Cardiac manifestations of subarachnoid hemorrhage. Expert Rev Cardiovasc Ther. 2011;9(3):303-7.

7. Karakike E, Moreno C, Gustot T. Infections in severe alcoholic hepatitis. Ann Gastroenterol. 2017;30(2):152-60.

8. Bernardini GL, Mayer SA. Subarachnoid Hemorrhage: Clinical Presentation and Neuropsychological Outcome. Medical Update for Psychiatrists. 1998;3(3):71-6.

9. Sabri M, Lass E, Macdonald RL. Early brain injury: a common mechanism in subarachnoid hemorrhage and global cerebral ischemia. Stroke Res Treat. 2013;2013:394036.

10. Etminan N. Aneurysmal subarachnoid hemorrhage--status quo and perspective. Transl Stroke Res. 2015;6(3):167-70.

11. Trojanowski T. How intracranial aneurysm rupture damages the brain. Interv Neuroradiol. 2008;14 Suppl 1(Suppl 1):9-12.

12. Yuksel S, Tosun YB, Cahill J, Solaroglu I. Early brain injury following aneurysmal subarachnoid hemorrhage: emphasis on cellular apoptosis. Turk Neurosurg. 2012;22(5):529-33.

13. Zhou Y, Martin RD, Zhang JH. Advances in experimental subarachnoid hemorrhage. Acta Neurochir Suppl. 2011;110(Pt 1):15-21.

14. Wu Y, Liu Y, Zhou C, Wu Y, Sun J, Gao X, et al. Biological Effects and Mechanisms of Caspases in Early Brain Injury after Subarachnoid Hemorrhage. Oxid Med Cell Longev. 2022;2022:3345637.

15. Fujii M, Yan J, Rolland WB, Soejima Y, Caner B, Zhang JH. Early brain injury, an evolving frontier in subarachnoid hemorrhage research. Transl Stroke Res. 2013;4(4):432-46.

16. Al-Tamimi YZ, Orsi NM, Quinn AC, Homer-Vanniasinkam S, Ross SA. A review of delayed ischemic neurologic deficit following aneurysmal subarachnoid hemorrhage: historical overview, current treatment, and pathophysiology. World Neurosurg. 2010;73(6):654-67.

17. Stein SC, Levine JM, Nagpal S, LeRoux PD. Vasospasm as the sole cause of cerebral ischemia: how strong is the evidence? Neurosurg Focus. 2006;21(3):E2.

18. Hou J, Zhang JH. Does prevention of vasospasm in subarachnoid hemorrhage improve clinical outcome? No. Stroke. 2013;44(6 Suppl 1):S34-6.

19. Cossu G, Messerer M, Oddo M, Daniel RT. To look beyond vasospasm in aneurysmal subarachnoid haemorrhage. Biomed Res Int. 2014;2014:628597.

20. Seule M, Muroi C, Sikorski C, Keller E. Monitoring of cerebral hemodynamics and oxygenation to detect delayed ischemic neurological deficit after aneurysmal subarachnoid hemorrhage. Acta Neurochir Suppl. 2013;115:57-61.

21. Yamaki VN, Cavalcanti DD, Figueiredo EG. Delayed Ischemic Neurologic Deficit after Aneurysmal Subarachnoid Hemorrhage. Asian J Neurosurg. 2019;14(3):641-7.

22. da Costa L, Fierstra J, Fisher JA, Mikulis DJ, Han JS, Tymianski M. BOLD MRI and early impairment of cerebrovascular reserve after aneurysmal subarachnoid hemorrhage. J Magn Reson Imaging. 2014;40(4):972-9.

23. Kronvall E, Undren P, Romner B, Saveland H, Cronqvist M, Nilsson OG. Nimodipine in aneurysmal subarachnoid hemorrhage: a randomized study of intravenous or peroral administration. J Neurosurg. 2009;110(1):58-63.

24. Ayer RE, Zhang JH. The clinical significance of acute brain injury in subarachnoid hemorrhage and opportunity for intervention. Acta Neurochir Suppl. 2008;105:179-84.

25. Sprague AH, Khalil RA. Inflammatory cytokines in vascular dysfunction and vascular disease. Biochem Pharmacol. 2009;78(6):539-52.

26. Tuttolomondo A, Pecoraro R, Pinto A. Studies of selective TNF inhibitors in the treatment of brain injury from stroke and trauma: a review of the evidence to date. Drug Des Devel Ther. 2014;8:2221-38.

27. Stanimirovic D, Satoh K. Inflammatory mediators of cerebral endothelium: a role in ischemic brain inflammation. Brain Pathol. 2000;10(1):113-26.

28. Jay GW, Dematttos RB, Weinstein EJ, Philbert MA, Pardo ID, Brown TP. Animal models for neural diseases. Toxicol Pathol. 2011;39(1):167-9.

29. Moor-Jankowski J, Goldsmith EI. The Laboratory for Experimental Medicine and Surgery in Primates. Ann N Y Acad Sci. 1969;162(1):324-8.

30. Mattison JA, Vaughan KL. An overview of nonhuman primates in aging research. Exp Gerontol. 2017;94:41-5.

31. Backer-Grondahl A, Lindal S, Lorentzen MA, Eldevik P, Vorren T, Kristiansen B, et al. A new non-craniotomy model of subarachnoid hemorrhage in the pig: a pilot study. Lab Anim. 2016;50(5):379-89.

32. Reinwald S, Burr D. Review of nonprimate, large animal models for osteoporosis research. J Bone Miner Res. 2008;23(9):1353-68.

33. Zhou ML, Shi JX, Zhu JQ, Hang CH, Mao L, Chen KF, et al. Comparison between one- and two-hemorrhage models of cerebral vasospasm in rabbits. J Neurosci Methods. 2007;159(2):318-24.

34. Kikkawa Y, Kurogi R, Sasaki T. The single and double blood injection rabbit subarachnoid hemorrhage model. Transl Stroke Res. 2015;6(1):88-97.

35. Pedard M, El Amki M, Lefevre-Scelles A, Compere V, Castel H. Double Direct Injection of Blood into the Cisterna Magna as a Model of Subarachnoid Hemorrhage. J Vis Exp. 2020(162).

36. Sabri M, Jeon H, Ai J, Tariq A, Shang X, Chen G, et al. Anterior circulation mouse model of subarachnoid hemorrhage. Brain Res. 2009;1295:179-85.

37. Altay T, Smithason S, Volokh N, Rasmussen PA, Ransohoff RM, Provencio JJ. A novel method for subarachnoid hemorrhage to induce vasospasm in mice. J Neurosci Methods. 2009;183(2):136-40.

38. Kamii H, Kato I, Kinouchi H, Chan PH, Epstein CJ, Akabane A, et al. Amelioration of vasospasm after subarachnoid hemorrhage in transgenic mice overexpressing CuZn-superoxide dismutase. Stroke. 1999;30(4):867-71; discussion 72.

39. Muroi C, Fujioka M, Marbacher S, Fandino J, Keller E, Iwasaki K, et al. Mouse model of subarachnoid hemorrhage: technical note on the filament perforation model. Acta Neurochir Suppl. 2015;120:315-20.

40. Zhao Y, Qu H, Wang Y, Xiao W, Zhang Y, Shi D. Small rodent models of atherosclerosis. Biomed Pharmacother. 2020;129:110426.

41. Ehret T, Torelli F, Klotz C, Pedersen AB, Seeber F. Translational Rodent Models for Research on Parasitic Protozoa-A Review of Confounders and Possibilities. Front Cell Infect Microbiol. 2017;7:238.

42. Alpdogan S, Li K, Sander T, Cornelius JF, Muhammad S. Cisterna Magna Injection Mouse Model of Subarachnoid Hemorrhage (SAH): A Systematic Literature Review of Preclinical SAH Research. Journal of Experimental Neurology. 2023;4(1):11-20.

43. Delgado TJ, Brismar J, Svendgaard NA. Subarachnoid haemorrhage in the rat: angiography and fluorescence microscopy of the major cerebral arteries. Stroke. 1985;16(4):595-602.

44. Guresir E, Raabe A, Jaiimsin A, Dias S, Raab P, Seifert V, et al. Histological evidence of delayed ischemic brain tissue damage in the rat double-hemorrhage model. J Neurol Sci. 2010;293(1-2):18-22.

45. Deacon RM. Measuring motor coordination in mice. J Vis Exp. 2013(75):e2609.

46. Osmon KJ, Vyas M, Woodley E, Thompson P, Walia JS. Battery of Behavioral Tests Assessing General Locomotion, Muscular Strength, and Coordination in Mice. J Vis Exp. 2018(131).

47. Brooks SP, Trueman RC, Dunnett SB. Assessment of Motor Coordination and Balance in Mice Using the Rotarod, Elevated Bridge, and Footprint Tests. Curr Protoc Mouse Biol. 2012;2(1):37-53.

48. Rustay NR, Wahlsten D, Crabbe JC. Assessment of genetic susceptibility to ethanol intoxication in mice. Proc Natl Acad Sci U S A. 2003;100(5):2917-22.

49. Deacon RM. Housing, husbandry and handling of rodents for behavioral experiments. Nat Protoc. 2006;1(2):936-46.

50. Gruen ME, Case BC, Foster ML, Lazarowski L, Fish RE, Landsberg G, et al. The Use of an Open Field Model to Assess Sound-Induced Fear and Anxiety Associated Behaviors in Labrador Retrievers. J Vet Behav. 2015;10(4):338-45.

51. Brenes JC, Padilla M, Fornaguera J. A detailed analysis of open-field habituation and behavioral and neurochemical antidepressant-like effects in postweaning enriched rats. Behav Brain Res. 2009;197(1):125-37.

52. Seibenhener ML, Wooten MC. Use of the Open Field Maze to measure locomotor and anxiety-like behavior in mice. J Vis Exp. 2015(96):e52434.

53. Marbacher S, Gruter B, Schopf S, Croci D, Nevzati E, D'Alonzo D, et al. Systematic Review of In Vivo Animal Models of Subarachnoid Hemorrhage: Species, Standard Parameters, and Outcomes. Transl Stroke Res. 2018.

54. Talbot SR, Biernot S, Bleich A, van Dijk RM, Ernst L, Hager C, et al. Defining body-weight reduction as a humane endpoint: a critical appraisal. Lab Anim. 2020;54(1):99-110.

55. Thal SC, Mebmer K, Schmid-Elsaesser R, Zausinger S. Neurological impairment in rats after subarachnoid hemorrhage--a comparison of functional tests. J Neurol Sci. 2008;268(1-2):150-9.

56. Garcia JH, Wagner S, Liu KF, Hu XJ. Neurological deficit and extent of neuronal necrosis attributable to middle cerebral artery occlusion in rats. Statistical validation. Stroke. 1995;26(4):627-34; discussion 35.

57. Bieber M, Gronewold J, Scharf AC, Schuhmann MK, Langhauser F, Hopp S, et al. Validity and Reliability of Neurological Scores in Mice Exposed to Middle Cerebral Artery Occlusion. Stroke. 2019;50(10):2875-82.

58. Kurtzke JF. Neurologic impairment in multiple sclerosis and the disability status scale. Acta Neurol Scand. 1970;46(4):493-512.

59. Pantoni L, Bartolini L, Pracucci G, Inzitari D. Interrater agreement on a simple neurological score in rats. Stroke. 1998;29(4):871-2.

60. Young LJ. The neurobiology of social recognition, approach, and avoidance. Biol Psychiatry. 2002;51(1):18-26.

61. Long B, Koyfman A, Runyon MS. Subarachnoid Hemorrhage: Updates in Diagnosis and Management. Emerg Med Clin North Am. 2017;35(4):803-24.

62. Du GJ, Lu G, Zheng ZY, Poon WS, Wong KC. Endovascular Perforation Murine Model of Subarachnoid Hemorrhage. Acta Neurochir Suppl. 2016;121:83-8.

63. Sugawara T, Ayer R, Jadhav V, Zhang JH. A new grading system evaluating bleeding scale in filament perforation subarachnoid hemorrhage rat model. J Neurosci Methods. 2008;167(2):327-34.

64. Gilli F, Royce DB, Pachner AR. Measuring Progressive Neurological Disability in a Mouse Model of Multiple Sclerosis. J Vis Exp. 2016(117).

65. Kraeuter AK, Guest PC, Sarnyai Z. The Open Field Test for Measuring Locomotor Activity and Anxiety-Like Behavior. Methods Mol Biol. 2019;1916:99-103.

66. Alpdogan S, Sander T, Zhang R, Khan D, Li X, Zhou H, et al. Meta-review on Perforation Model of Subarachnoid Hemorrhage in Mice: Filament Material as a Possible Moderator of Mortality. Transl Stroke Res. 2022.

67. Locksley HB, Sahs AL, Sandler R. Report on the cooperative study of intracranial aneurysms and subarachnoid hemorrhage. 3. Subarachnoid hemorrhage

unrelated to intracranial aneurysm and A-V malformation. A study of associated diseases and prognosis. J Neurosurg. 1966;24(6):1034-56.

68. Roquer J, Cuadrado-Godia E, Guimaraens L, Conesa G, Rodriguez-Campello A, Capellades J, et al. Short- and long-term outcome of patients with aneurysmal subarachnoid hemorrhage. Neurology. 2020;95(13):e1819-e29.

69. Roa JA, Sarkar D, Zanaty M, Hasan D, Samaniego E, Ortega SB. Abstract TP454: Immunological Responses in Patients With Vasospasm After Aneurysmal Subarachnoid Hemorrhage: A Pilot Study. Stroke. 2020;51(Suppl_1).

70. Paisan GM, Ding D, Starke RM, Crowley RW, Liu KC. Shunt-Dependent Hydrocephalus After Aneurysmal Subarachnoid Hemorrhage: Predictors and Long-Term Functional Outcomes. Neurosurgery. 2018;83(3):393-402.

71. Titova E, Ostrowski RP, Zhang JH, Tang J. Experimental models of subarachnoid hemorrhage for studies of cerebral vasospasm. Neurol Res. 2009;31(6):568-81.

72. Longa EZ, Weinstein PR, Carlson S, Cummins R. Reversible middle cerebral artery occlusion without craniectomy in rats. Stroke. 1989;20(1):84-91.

73. Muroi C, Fujioka M, Okuchi K, Fandino J, Keller E, Sakamoto Y, et al. Filament perforation model for mouse subarachnoid hemorrhage: surgical-technical considerations. Br J Neurosurg. 2014;28(6):722-32.

74. Feiler S, Friedrich B, Scholler K, Thal SC, Plesnila N. Standardized induction of subarachnoid hemorrhage in mice by intracranial pressure monitoring. J Neurosci Methods. 2010;190(2):164-70.

75. Peng J, Wu Y, Pang J, Sun X, Chen L, Chen Y, et al. Single clip: An improvement of the filament-perforation mouse subarachnoid haemorrhage model. Brain Inj. 2019;33(6):701-11.

76. Chiu JJ, Usami S, Chien S. Vascular endothelial responses to altered shear stress: pathologic implications for atherosclerosis. Ann Med. 2009;41(1):19-28.

77. Shi ZD, Tarbell JM. Fluid flow mechanotransduction in vascular smooth muscle cells and fibroblasts. Ann Biomed Eng. 2011;39(6):1608-19.

78. Seldinger SI. Catheter replacement of the needle in percutaneous arteriography; a new technique. Acta radiol. 1953;39(5):368-76.

79. Lin CL, Calisaneller T, Ukita N, Dumont AS, Kassell NF, Lee KS. A murine model of subarachnoid hemorrhage-induced cerebral vasospasm. J Neurosci Methods. 2003;123(1):89-97.

80. Attia MS, Loch Macdonald R. Anterior circulation model of subarachnoid hemorrhage in mice. Acta Neurochir Suppl. 2015;120:311-4.

81. Mielke D, Bleuel K, Stadelmann C, Rohde V, Malinova V. The ESAS-score: A histological severity grading system of subarachnoid hemorrhage using the modified double hemorrhage model in rats. PLoS One. 2020;15(2):e0227349.

82. Liu S, Tielking K, von Wedel D, Nieminen-Kelha M, Mueller S, Boehm-Sturm P, et al. Endovascular Perforation Model for Subarachnoid Hemorrhage Combined with Magnetic Resonance Imaging (MRI). J Vis Exp. 2021(178).

83. Miyaoka R, Yamamoto J, Miyachi H, Suzuki K, Saito T, Nakano Y. Intra-arterial Contrast-enhanced Micro-computed Tomography Can Evaluate Intracranial Status in the Ultra-early Phase of Experimental Subarachnoid Hemorrhage in Rats. Neurol Med Chir (Tokyo). 2021;61(12):721-30.

84. Shishido H, Egashira Y, Okubo S, Zhang H, Hua Y, Keep RF, et al. A magnetic resonance imaging grading system for subarachnoid hemorrhage severity in a rat model. J Neurosci Methods. 2015;243:115-9.

85. Hunt WE, Hess RM. Surgical risk as related to time of intervention in the repair of intracranial aneurysms. J Neurosurg. 1968;28(1):14-20.

86. Teasdale G, Jennett B. Assessment of coma and impaired consciousness. A practical scale. Lancet. 1974;2(7872):81-4.

87. Schwartz AY, Masago A, Sehba FA, Bederson JB. Experimental models of subarachnoid hemorrhage in the rat: a refinement of the endovascular filament model. J Neurosci Methods. 2000;96(2):161-7.

6. Appendix

Video. 1: Surgical Procedure of Puncture Technique Application in Circle Willis Perforation Subarachnoid Hemorrhage Mouse Model.

Video Link: https://youtu.be/yGFJJISvkg

7. Acknowledgement

I extend my deepest appreciation to PD Dr Med. Sajjad Muhammad, whose unwavering guidance and expertise have profoundly influenced my research journey. His consistent support and insightful feedback have been invaluable, shaping both my academic and personal growth. I am grateful to Prof. Jan Frederick Cornelius and Prof. Danial Hänggi for their encouragement and support during my doctoral studies at the Department of Neurosurgery, University Hospital Düsseldorf. Special thanks to my second supervisor, Majeed Rana, for his scientific mentorship throughout this project.

I am indebted to Dr. Dilaware Khan for his exceptional assistance and expertise. His patience and willingness to share knowledge have greatly contributed to the success of this project, providing valuable insights and constructive criticism. I express heartfelt gratitude to my parents, Prof. Bingjin Zhang and Mrs. Haixiu Liu, and my partner, Dr. Shuang Liu, whose unwavering love and support have been my pillars of strength. I am also thankful for the love, encouragement, and sacrifices of my daughters, Zixuan Zhang and Mingxuan Zhang, who have been constant sources of motivation.

Furthermore, I acknowledge the collaboration of Prof. Timm Filler from the Department of Anatomy, as well as the support from colleagues at the Animal Department (ZETT), including Mr Michael Hewera, Dr. Xuanchen Li, and Dr. Huakang Zhou. Their assistance, insightful discussions, and conducive work environment have been integral to the progress of this project.